THE JOURNAL OF PHYSICAL CHEMISTRY B

Article

Solubility of Sugars and Sugar Alcohols in Ionic Liquids: Measurement and PC-SAFT Modeling

Aristides Pinto Carneiro, Christoph Held, Oscar Rodriguez, Gabriele Sadowski, and Maria Eugénia Rebello Almeida Macedo

J. Phys. Chem. B, **Just Accepted Manuscript** • DOI: 10.1021/jp404864c • Publication Date (Web): 30 Jul 2013

Solubility of sugars and sugar alcohols in ionic liquids: measurement and PC-SAFT modeling

Aristides P. Carneiro [a], *Christoph Held* [*,b], *Oscar Rodríguez* [a,†], *Gabriele Sadowski* [b], *Eugénia A. Macedo* [a]

[a] LSRE – Laboratory of Separation and Reaction Engineering – Associate Laboratory LSRE/LCM, Faculdade de Engenharia, Universidade do Porto, Rua Dr. Roberto Frias, 4200-465 Porto, Portugal

[b] Laboratory of Thermodynamics, Department of Biochemical and Chemical Engineering, Technische Universität Dortmund, Emil-Figge-Str. 70, 44227 Dortmund, Germany

[†] *Present address:* Department of Chemical Engineering, University of Santiago de Compostela, Spain.

Abstract

Biorefining processes using ionic liquids (ILs) require proper solubility data of biomass-based compounds in ILs, as well as an appropriate thermodynamic approach for the modeling of such data. Carbohydrates and their derivatives such as sugar alcohols represent a class of compounds that could play an important role in biorefining. Thus, in this work pure-IL density and solubility of xylitol and sorbitol in five different ILs were measured between 288 and 339 K. The ILs under consideration were: 1-ethyl-3-methylimidazolium dicyanamide, 1-butyl-3-methylimidazolium dicyanamide, Aliquat® dicyanamide, trihexyltetradecylphosphonium dicyanamide, and 1-ethyl-3-methylimidazolium trifluoroacetate. Comparison with the literature data was performed, showing good agreement. With the exception of [bmim][DCA], the solubility of these sugar alcohols in the other ILs is presented for the first time. The measured data as well as previously published solubility data of glucose and fructose in these ILs were modeled by means of PC-SAFT using a molecular-based associative approach for ILs. PC-SAFT was used in this work as it has shown to be applicable to model the solubility of xylitol and sorbitol in ILs (Paduszyński et al., J. *Phys.Chem. B* 117, 7034-7046, 2013). For this purpose, three pure-IL parameters were fitted to pure-IL density, activity coefficients of 1-propanol at infinite dilution in ILs, and/or xylitol solubility in ILs. This approach allows accurate modeling of the pure-IL data and the mixture data with only one binary interaction parameter k_{ij} between sugar and IL or sugar alcohol and IL. In cases where only pure-IL density and activity coefficients of 1-propanol at infinite dilution in ILs were used for the IL-parameter estimation, the solubility of sugars and sugar alcohols in ILs could be predicted (k_{ij}=0 between sugar and IL or sugar alcohol and IL) with reasonable accuracy.

Keywords: sugars, sugar alcohol, ionic liquids, solubility, PC-SAFT, modeling, prediction

** corresponding author: Christoph.Held@bci.tu-dortmund.de*

1. Introduction

It is common sense that future sustainability depends on the exploitation of alternative sources for energy and chemicals. Biomass-derived sugars and sugar alcohols (both referred to as “sugars” in the following) are potential precursors of commodity chemicals and added-value compounds[1]. Processing biomass in a biorefinery requires suitable solvents, which are able to dissolve biomass, catalyze the hydrolysis of the main polysaccharides (cellulose and hemicellulose) to sugars, and promote the transformation of sugars into intermediate chemicals or final products. Ionic liquids (ILs), a still recent class of "molten salts", have been extensively applied in academia as suitable solvents for many applications in a broad spectrum of fields (e.g. [2-4]). Their unique properties [5-7], mainly the so-called "non-volatility" and high thermal stability, made them attractive tools to face many operatory challenges. Their versatility allows the properties to be "tailored" by choosing an appropriate anion-cation pair. Thus, an IL can be designed according to the physical or chemical demands for a given application. In biomass processing, ILs have been successfully applied as solvent media, extraction agents, as well as catalysts for several reactions [8,9]. The main advantage of their use in biorefining is the fact that ILs can either dissolve the whole biomass[10,11] or dissolve the main polysaccharides (cellulose, hemicellulose and lignin) selectively[12]. In addition, dissolution and hydrolysis reactions can be performed in relatively mild conditions[13,14] when compared to standard processes for biomass pretreatment and hydrolysis (alkali pretreatment, acidic hydrolysis, steam explosion, pyrolysis, etc.). Furthermore, ILs can improve the conversion and the selectivity of several sugar reactions [15,16].

Phase-equilibrium data as well as their modeling are of key relevance for designing biorefining processes involving ILs as solvents. Especially solubility data are needed to design separation and reaction units. Different experimental procedures have been applied to measure solubility of sugars or sugar alcohols in ILs [17-23]. Most of them use an approach in which the solubility is obtained at constant temperature (isothermal approach) [17-22,24]. To ensure that equilibrium is reached, usually incremental amounts of the sugar component are added to an IL, until saturation is reached[17,20,21]. Another method consists in adding an excess of sugar to the IL [22,25] and

measure the sugar concentration of the IL solution over the time until saturation (no variation in sugar concentration). Another possible approach is to measure the equilibrium temperature at constant composition (polythermal approach). Sugar solubility data in ILs are still scarce in literature, and in most of the studies the data are available only at a single temperature. Moreover, the available literature data cover essentially only the most well-known sugars: glucose, fructose, and sucrose as well as polysaccharides such as cellulose. Our previous works in this field [22,25,26] aimed to close this gap of data, providing accurate solubilities in ILs within a broad range of temperature. Regarding experimental solubility of sugar alcohols in ILs, Payne and Kerton[27] were the pioneers, reporting solubility of xylitol in two ILs at 373 K. In 2011, Conceição et al.[23] measured the solubilities of mannitol and xylitol in 10 ILs in a wide range of temperature. Later on, our group published solubility of xylitol and sorbitol in three ILs in the temperature range 288-343 K[25]. More recently, Paduszyński et al.[24] reported solubility of xylitol and sorbitol in dicyanamide-based ILs. Special care has to be given to the fact that ILs are highly-hygroscopic compounds. In addition, the solubility of sugar-like compounds is strongly affected by the presence of water in ILs[21,28]. This requires keeping the water content in ILs as low as possible and further measuring and reporting the amount of water in ILs prior and after their use.

Thermodynamic models used to describe and predict properties and phase equilibria of mixtures containing sugars and ILs have to account for several specific interactions. Correlation of those data has already been performed[22,25,26] by means of local composition models such as NRTL[29] and UNIQUAC[30]. SAFT-based equations of state (EoS) were recently applied to model sugar/water systems. Feng et al. [31] used original SAFT [32] to represent water activity in sugar solutions and solubility of glucose, fructose, and sucrose in water. To obtain the sugar pure-component parameters, the authors used the critical point and normal boiling temperature of the sugar, which they calculated using group contribution methods. In a second step, they modeled the sugar solubility in water by fitting quadratic temperature-dependent k_{ij} values. This shortcoming was probably caused by inappropriate pure-component parameters. Later, Ji et al.[33] also used SAFT and the same parameter-estimation procedure to predict the density of aqueous sugar solutions. In a following work, the same research

group published the use of SAFT for modeling water activities, mixture densities, and oxygen solubilities in sugar alcohol solutions [34]. They applied four association sites for all sugars and three association sites for water.

In our previous work[35] we demonstrated that PC-SAFT is suitable to model sugars in aqueous and non-aqueous solutions. The association scheme for each sugar was chosen according to its molecular structure (i.e. number of OH groups). Using only four adjustable parameters, which were fitted to aqueous-solution density and osmotic-coefficient data, PC-SAFT was able to predict satisfactorily sugar and sugar alcohol solubility in single and mixed solvents and even in multi-solute sugar systems.

Besides these works on sugar modeling, ILs have also been modeled extensively with SAFT-based EoS. Two excellent and complete reviews [36,37] containing the main research on modeling IL systems, including cubic and molecular-based equations of state as well as molecular dynamics studies, also report the use of SAFT-based approaches. Kroon et al.[38] were the pioneers applying SAFT to systems containing ILs. They used the tPC-PSAFT EoS to model solubilities of CO_2 in ILs. Many other versions of SAFT were also applied to systems with ILs, e.g. PC-SAFT[39-41], Soft-SAFT[42], SAFT-gamma[43], SAFT-VR[44], and hetero-SAFT[45]. They differ among each other in the reference-fluid system, in the combining rules for fluid mixtures, and in the kind of molecular interactions which are taken into account. It is also noteworthy to mention that in SAFT-based models, the ILs can be treated as homo-segmented or hetero-segmented molecules, or as fully dissociated species (ePC-SAFT). The original version of PC-SAFT has been used for modeling many mixtures with ILs, e.g. the solubility of CO_2 in imidazolium-based ILs[39-41]. In a recent work[41] ILs were treated as homo-segmented non-dissociated species and only three parameters (segment number, diameter and dispersion energy) were fitted to experimental pure-IL density. The association parameters were kept constant (equal to those of 1-alkanols). Two association sites of type B and one site of type A were considered for each IL and only AB interactions were allowed. Temperature-independent k_{ij} values were fitted to binary data to correlate CO_2 solubilities with good accuracy. In a similar way, Rahmati-Rostami et al. [44] used PC-SAFT to model the solubility of hydrogen sulfide in imidazolium-based ILs containing the anions $[BF_4]^-$, $[PF_6]^-$, and $[NTf_2]^-$. Another

approach for the description of CO_2 and CH_4 solubility in ILs was proposed by Ji et al. [46] who used the PC-SAFT model assuming either complete dissociation of the IL into ions (ion based approach , ePC-SAFT) or non-dissociation (molecular based approach). Therewith, quantitative gas solubility predictions in ILs were possible over a wide range of pressure and temperature. Recently, Domańska et al. [40] applied PC-SAFT using a 10-site association scheme for ILs to model binary mixtures containing isoquinolinium-based ILs and an organic solvents. The pure-IL parameters were fitted to IL density and Hildebrand solubility parameters. Paduszyński and Domańska [47] modelled the solubility of aliphatic hydrocarbons in piperidinium ILs. They proposed the use of infinite-dilution activity coefficients for fitting temperature-dependent binary interaction parameters, while the pure-component parameters were fitted to pure-IL density data and IL-solubility data that were determined from Hildebrand parameters at different temperatures. Nann et al.[39] showed that pure-IL densities and activity-coefficient data (in this case 1-butanol) are appropriate data for the estimation of pure-IL PC-SAFT parameters. Very recently, the solubility of sugar-like molecules in ILs was modeled for the very first time using PC-SAFT by Paduszyński et al.[24] Therein ILs were modeled with a symmetric 6-site association scheme. The pure-component parameters for [bmim][DCA] were fitted to experimental atmospheric liquid-density data and vapor-pressure data of pure IL. The other two dicyanamide-based ILs in that work were modeled with the same association scheme and just the segment number, m_i^{seg}, and segment diameter, σ_i, were fitted to density of those ILs, being the remaining parameters (ui/kB, ε^{AiBi}/k_B and κ^{AiBi}) transferred from [bmim][DCA]. For the sugar alcohols a 2B scheme for each OH group was assigned and pure-component parameters were fitted to liquid-density data and vapor-pressure data of pure sugar alcohols at elevated temperatures. With this strategy, the authors obtained a good solubility modeling applying k_{ij} values for dispersion and association energy.

In this work, experimental solubility data of xylitol and sorbitol in five ILs are presented. Four dicyanamide ILs and one trifluoroacetate IL were used in this work: 1-ethyl-3-methylimidazolium dicyanamide [emim][DCA], 1-butyl-3-methylimidazolium dicyanamide [bmim][DCA], Aliquat®[DCA], trihexyltetradecylphosphonium dicyanamide [$P_{6,6,6,14}$][DCA], and 1-ethyl-3-methylimidazolium trifluoroacetate [emim][TFA]. The

pure-component densities of these ILs were measured and compared with literature values. Original PC-SAFT [48] was applied to model solubility data of sugars (glucose and fructose) and sugar alcohols (xylitol and sorbitol) in these ILs. An additional IL, [emim][$EtSO_4$], was also considered herein for the modeling results. Two different approaches for the PC-SAFT IL-parameter estimation are presented. In a first approach, pure-IL density and activity coefficients at infinite dilution of 1-propanol in the ILs were used. A different parameter-estimation procedure was applied to ILs for which experimental 1-propanol activity-coefficient data at infinite dilution were not available: parameters were fitted to pure-IL density and solubility of xylitol in these ILs. Experimental solubility data and modeling results obtained for systems with [bmim][DCA] were compared to those published by Paduszyński et al.[24].

2. Experiments

Materials

The ILs 1-ethyl-3-methylimidazolium dicyanamide, [emim][DCA] (> 99 wt%), 1-butyl-3-methylimidazolium dicyanamide, [bmim][DCA] (> 98 wt%) and trihexyltetradecylphosphonium dicyanamide, [$P_{6,6,6,14}$][DCA] (> 95 wt%) were supplied by Iolitec GmbH (Germany) and used without further purification. Xylitol (99 wt%, Alfa Aesar) and D (-) sorbitol (99.9 wt%, Merck KGaA, Germany) were the sugar alcohols used in this work. They were dried under vacuum prior to the measurements. The chemicals needed for the synthesis of 1-ethyl-3-methylimidazolium trifluoroacetate were ethyl trifluoroacetate (>99.9 wt%, Merck KGaA, Germany) and 1-methylimidazole (>99 wt%, Merck KGaA, Germany). Sodium dicyanamide (>97 wt%, Acros Organics) and Aliquat®336[a] with 3.86 wt% of water (measured by Karl-Fisher titration in this work) and with an average molecular weight of 442 $g \cdot mol^{-1}$ were supplied by Acros Organics and used to synthesize Aliquat®[DCA]. Other chemicals such as toluene (>99.99 wt%, Fisher Scientific), acetone (>99.9 wt%, Labsolve), n-heptane (>99 wt%, BDH Prolabo), and dichloromethane (99.99 wt% Fisher Scientific) were needed for the synthesis. Silver nitrate, $AgNO_3$ (*Ph. Eur*, Merck KGaA, Germany) was used for the quantification of chloride content in Aliquat®[DCA].

[a]Aliquat®336 is a commercial name for a chloride ionic liquid with a mixture of the cations: trioctylmethylammonium and tridecylmethylammonium, predominating the former (0.55 of mole fraction).

The chemical structures of the ion species of the ILs considered in this work are illustrated in Figure 1.

Synthesis of [emim][TFA]

A solvent-free reaction was carried out to produce [emim][TFA] according to the literature[49]. Roughly 9 g of 1-methylimidazole and 16 g of ethyl trifluoroacetate were mixed in a closed stainless steel reactor at 373 K. The mixture was stirred for 24 h, and the unconverted reactants were removed under vacuum. The obtained [emim][TFA] contained 1200 ppm of water (measured by Karl-Fisher titration) and the chemical structure of [emim][TFA] was checked by ^{1}H NMR. Detailed information about this synthesis is available in a previous publication[26].

Synthesis of Aliquat®[DCA]

The metathesis reaction between Aliquat®336 and sodium dicyanamide for anion exchange was performed according to a literature procedure[50]. A mixture of the two reactants (with 25% molar excess of sodium dicyanamide) in dichloromethane was stirred for 48h. Then, the suspension was filtered and the obtained liquid was distilled to remove the excess of dichloromethane. Vacuum was applied to purify the IL, and a final water content of 500 ppm was determined by Karl-Fisher titration. The final chloride content was found to be lower than 1300 ppm (measured by Mohr's method). The cation structure was verified through ^{1}H NMR. Further detailed information about this synthesis is available in a previous publication[26].

Solubility measurement of the sugar alcohols in the ILs

An isothermal technique was applied to determine the sugar alcohol solubilities in ILs. In this procedure, 25 mL-jacketed equilibrium cells were used, in which roughly 10 g of the IL were placed together with a given amount of sugar alcohol. Water from a

JULABO F12-ED recirculation bath (Julabo, USA) was pumped through the cell jacket in order to keep a constant temperature in the inner cell with a precision of ± 0.1 K. The binary mixture was magnetically stirred until equilibrium was reached. The system was supervised to ensure that a solid phase was present during equilibration. In order to evaluate whether the system reached the equilibrium state or not, samples were drawn at different dissolution times, and the concentration of the sugar alcohol was measured. At the point where no variation in sugar alcohol concentration was observed, the saturation equilibrium was assumed to be reached. Hence, this measured concentration corresponded to the solubility concentration. Before each sampling, the stirring was stopped and phase separation took place until the whole solid phase was settled down in the cell. Sampling was made in triplicate and the sugar alcohol concentrations were quantified by HPLC (LaChrom Elite®, HITAKI, USA). A 250×4 mm HPLC column with Purospher®STAR RP-18e (5µm) as stationary phase was used. An isocratic method with water as eluent and a flow of 0.7 $mL \cdot min^{-1}$ was chosen. Sugar alcohol detection was carried out with continuous refractive index measurement at 313 K.

Density of the pure ILs

Densities of the ILs [emim][DCA], [bmim][DCA], [emim][TFA], Aliquat®[DCA], and $[P_{6,6,6,14}]$[DCA] were measured between 278 - 343 K. The apparatus used was a vibrating-tube densimeter DMA 4500 M (Anton Paar, Germany) with a precision of ± 0.00001 $g \cdot cm^{-3}$ for density and ±0.01K for temperature.

3. Modeling

3.1. PC-SAFT equation of state

The PC-SAFT model was developed based on a perturbation theory using the hard-chain fluid as the reference fluid system. The model assumes molecules as being chains of spherical segments. Specific interactions such as hydrogen bonding between molecules are described by considering association sites on the segments. PC-SAFT

calculates the reduced residual Helmholtz energy of a system (a^{res}) as a sum of the reference-chain contribution (a^{hc}), dispersive interactions (a^{disp}), and association (a^{assoc}) effects:

$$a^{res} = a^{hc} + a^{disp} + a^{assoc} \quad (1)$$

The hard-chain term, a^{hc}, is the reference contribution in which only repulsive interactions are taken into account. The non-spherical shape of the molecules is also considered in this term, by portraying the molecules as chains of spherical segments - hard-chain fluid. Then a dispersive term, a^{disp}, resulting from the application of a second order perturbation theory to the hard-chain reference system is added to account for attractive interactions between the chains through dispersive forces. Specific interactions such as association (i.e. hydrogen bonding) are considered in the associative term, a^{assoc}, in which the magnitude of these interactions is measured by the association strength between donor and acceptor sites which are assigned to each molecule. Other contributions such as polar or Coulomb interactions can be also taken into account but were not considered herein. In this work, the ILs and the sugars were described as non-dissociated molecules. Self-association was considered for both sugars and ILs as it is well-known that these molecules interact strongly through hydrogen bonding. In concentrated solutions, ILs are often considered to be present as non-dissociated molecules using SAFT-based modeling approaches[47,51]. As this work deals with those solutions, IL dissociation and Coulomb forces due to charges were neglected. In addition, there are experimental and theoretical evidences that ILs and carbohydrates interact essentially through hydrogen bonding[52,53]. Thus, a polar term was not considered. Such term would also increase the complexity of the model, requiring the knowledge of dipolar moments for ILs or the fitting of additional parameters. As for ion pairing, this is accounted within the association term of PC-SAFT. The expressions to calculate the reduced residual Helmholtz energy contributions of Eq.(1) are those used in the original PC-SAFT[48]. In general, five pure-component parameters are required to describe an associating compound: the number of segments m_i^{seg}, the diameter of the segments σ_i, the van der Waals-interaction (dispersion) energy parameter between segments of two different molecules u_i/k_B, and two additional parameters to account for association between

acceptor sites A_i and donor sites B_i, namely the association-energy parameter ε^{AiBi}/k_B and the association-volume parameter κ^{AiBi}. Moreover, the number of association sites in each compound must be set prior to the parameter estimation. To handle fluid mixtures, the conventional Berthelot-Lorentz combining rules were used to calculate the mixture parameters:

$$\sigma_{ij} = \frac{1}{2}(\sigma_i + \sigma_j) \tag{2}$$

$$u_{ij} = (1 - k_{ij})\sqrt{u_i u_j} \tag{3}$$

The binary interaction parameter k_{ij} in Eq.(3) was introduced to correct the dispersive energy between two components. This parameter is usually obtained by fitting to binary experimental data such as activity coefficients or solubilities. Keeping k_{ij}=0, the predictive form (no binary data used) of the model is conserved. To account for cross association between a sugar and an IL, the combining rules proposed by Wolbach and Sandler[54] were used in this work:

$$\varepsilon^{A_iB_j} = \frac{1}{2}(\varepsilon^{A_iB_i} + \varepsilon^{A_jB_j}) \tag{4}$$

$$\kappa^{A_iB_j} = \sqrt{\kappa^{A_iB_i}\kappa^{A_jB_j}}\left(\frac{\sqrt{\sigma_i\sigma_j}}{{}^{1}/_{2}(\sigma_i+\sigma_j)}\right)^3 \tag{5}$$

3.2 Calculation of thermodynamic properties with PC-SAFT

Various physical and thermodynamic properties can be obtained from the residual Helmholtz energy. First, the compressibility factor, Z is calculated from PC-SAFT as a derivative of a^{res} with respect to density, ρ :

$$Z(\rho) = 1 + \rho\left(\frac{\partial a^{res}}{\partial \rho}\right)_{T,x} \tag{6}$$

where x stands for the composition of the mixture and T for the temperature.

For density calculations, Eq.(7) has to be solved:

$$p - \rho RTZ(\rho) = 0 \tag{7}$$

where R is the ideal gas constant (8.314 J·mol·K^{-1}) and p the system pressure. Herein, the density roots are obtained iteratively at given temperature and pressure.

The fugacity coefficient φ_i of component i can be obtained as follows:

$$\ln \varphi_i = (Z-1) - \ln Z + a^{res} + \frac{\partial a^{res}}{\partial x_i} - \sum_i x_i \frac{\partial a^{res}}{\partial x_i} \quad (8)$$

Activity coefficients γ_1^{∞} of component 1 at infinite dilution in component 2 can be calculated from the fugacity coefficients:

$$\gamma_1^{\infty} = \frac{\varphi_1^{\infty}(T,p)}{\varphi_{01}(T,p)} \quad (9)$$

where 0 and ∞ stands for pure-compound state and infinite dilution, respectively. Considering a binary mixture of a volatile (1) and a non-volatile (2) component, the osmotic coefficient ϕ of this mixture can be obtained from the knowledge of fugacity coefficients of component 1:

$$\phi = -\frac{1000\, ln\left(x_1 \frac{\varphi_1}{\varphi_{01}}\right)}{m_2 M_1} \quad (10)$$

with m_2 and M_1 being the molality of a non-volatile component 2 in (moles of 2 per kg of pure 1) and the molecular weight of the volatile component 1 in (g/mol), respectively

In order to calculate the solubility x_i (in mole fraction) of a component i in a liquid, the following solid-liquid equilibrium condition [55] was applied in this work:

$$\ln\left(x_i \cdot \frac{\varphi_i}{\varphi_{0i}{}^{L}}\right) = \frac{\Delta H_{0i}^{S-L}}{R T_{0i}^{S-L}}\left(1 - \frac{T_{0i}^{S-L}}{T}\right) - \frac{\Delta C_{p,i}^{S-L}}{R}\left[\left(1 - \frac{T_{0i}^{S-L}}{T}\right) + \ln\left(\frac{T_{0i}^{S-L}}{T}\right)\right] \quad (11)$$

In Eq.(11), the subscript i stands for a sugar component in this work and $\Delta H_{0i}{}^{S\text{-}L}$, $T_{0i}{}^{S\text{-}L}$, and $\Delta c_{p,i}{}^{S\text{-}L}$ are the melting enthalpy, melting temperature, and heat-capacity difference of the pure sugar between its solid and its (hypothetical) liquid state, respectively. $\varphi_{0i}{}^{L}$ and φ_i stand for the sugar fugacity coefficient as pure subcooled liquid (hypothetical state) and in the liquid mixture, respectively. Solubility data and modeling results are presented in this work in molality, i.e. moles sugar per kg pure IL. Mole fractions of sugars x_2 were converted to molality m_2 using the molar mass of IL M_1 according to

$$m_2 = \frac{1000x_2}{M_1x_1} \quad (12)$$

3.3. Parameter estimation

Modeling a sugar+IL mixture requires PC-SAFT parameters for the pure IL, the pure sugar, and binary interaction parameters k_{ij}. Due to their non-volatile character, ionic liquids and sugars can hardly be parameterized using pure liquid densities and pure vapor pressures. Moreover, sugars do not exist as pure liquids. Therefore, alternative parameter estimation strategies are needed to model systems containing these compounds.

i) Sugar parameters

The sugar parameters were taken from a previous work[35]. They were obtained by adjusting four parameters: m_i^{seg}, σ_i, u_i/k_B, and a binary k_{ij} between sugar and water to experimental aqueous-solution densities and osmotic coefficients at 298 K. The association-energy and association volume parameters were set to constant values. The association scheme was set according to the number of hydroxyl groups present in the solutes. These parameters allowed for satisfactory solubility predictions in water as well as in solvent mixtures (e.g. water/alcohol). Therefore, they were also applied in this work although the solvent is an IL instead of water. Table 1 presents these pure-component parameters for the sugars and sugar alcohols considered herein as well as their melting properties which were taken from literature.

ii) IL parameters

To obtain the PC-SAFT parameters for ILs pure-IL density data are appropriate. However, fitting to volumetric data alone is often not sufficient for estimating energy parameters such as u_i/k_B. Therefore, additional experimental data are necessary to provide a set of parameters that represents well both the volumetric and the energetic properties of the ILs. In general, vapor-pressure data of pure ILs would be appropriate for the pure-IL parameter estimation. However, such data are difficult to measure with high precision and are available only for very limited set of ILs. Due to this fact, the use of binary experimental data is a valid option, e.g. osmotic coefficients of water/IL or alcohol/IL solutions[63-65]. However, the limited maximum IL concentration (e.g. < 5

mol·kg^{-1} in vapor-pressure osmometry experiments) may not be appropriate to model systems with very high IL contents. Another possibility is the use of activity coefficients of alcohol at infinite dilution in ILs [39,47]. These data are more suitable to describe systems at high (nearly pure) IL concentrations.

In this work, two strategies for the estimation of pure-IL parameters were applied. In the first strategy, pure-IL densities and infinite-dilution activity coefficients of 1-propanol in ILs were used. A second strategy was applied to systems for which these data were not available; in this second strategy IL parameters were fitted to pure-IL densities and xylitol solubilities in ILs. This approach is expected to provide good correlating results for sugar solubility, but may have limitations when using the IL parameters for prediction of other (solubility-independent) thermodynamic data.

Independent of the strategy, the following objective function, OF, was minimized in the parameter estimation:

$$\mathrm{OF} = \log_{10}\left(\frac{\sum_{i=1}^{N_{data}}\left(1-\frac{Y_i^{PC-SAFT}}{Y_i^{exp.}}\right)^2}{N_{data}}\right) \tag{13}$$

where N_{data} is the total number of experimental points used and Y refers to a generic property, being pure-IL density, alcohol activity coefficient at infinite dilution, or sugar solubility in IL in this work.

IL parameter estimation: strategy 1

The ILs [emim][EtSO$_4$], [emim][DCA], and [emim][TFA] were parameterized using pure-IL density and activity-coefficient data at infinite dilution γ_{1-p}^{∞} of 1-propanol (component 1) in these ILs (component 2). Reasons for choosing these data was their availability in the literature and the fact that sugars and alcohols are similar with respect to the interactions they can exhibit: both are able to self-associate and cross-associate and further have apolar parts. In this work, preliminary studies were carried out using experimental pure-IL densities together with experimental alcohol activity coefficients at infinite dilution for the IL-parameter estimation. Comparing the use of ethanol, 1-propanol, or 1-butanol activity coefficients at infinite dilution these studies showed that using the so-determined pure-IL parameters yield a similar performance for sugar solubility predictions, independent of the alcohol chosen for the γ_1^{∞} data.

Due to the fact that experimental 1-propanol activity coefficients at infinite dilution were available for the largest number of ILs investigated in this work, 1-propanol was the alcohol chosen for γ_1^∞ data to be used in the parameter estimation.

The temperature range for the chosen values of γ_{1-p}^∞ was set according to the temperature range (288 - 339 K) of solubility data. Besides γ_{1-p}^∞ data also experimental pure-IL densities stemming from this work and from literature were used for the parameter estimation. According to our previous work[46], the association parameters for ILs were set to ε^{AiBi}/k_B = 5000 K and κ^{AiBI} = 0.1 as these values had been found to be appropriate to model densities of imidazolium-based ILs. The k_{ij} values between ILs and 1-propanol were set to zero, according to a previous research conducted by us[39]. Thus, only three adjustable IL parameters were determined using this strategy, namely m_i^{seg}, σ_i , and u_i/k_B.

Different association schemes for each IL were tested in order to determine the scheme which yields the highest overall accuracy with respect to IL-density, activity coefficient γ_{1-p}^∞, and sugar solubility (in terms of ARD, see Eq.(14)). Symmetric association schemes (number of donor sites equal to the number of acceptor sites) with the total number of association sites ranging between 2 (1+1) and 10 (5+5) were applied in these preliminary analyses. Table 2 summarizes the obtained parameters for the ILs with the best association scheme, and the average relative deviations (ARDs) for density and γ_{1-p}^∞. These ARDs were calculated by:

$$ARD(\%) = \frac{100}{N_{data}} \sum_{i=1}^{N_{data}} \frac{|Y_i^{exp.} - Y_i^{PC-SAFT}|}{Y_i^{exp.}} \quad (14)$$

where Y refers to pure-IL density, γ_{1-p}^∞ , or sugar solubility in the IL .

IL parameter estimation: strategy 2

For the other three ILs investigated in this work ([bmim][DCA], Aliquat[DCA], and [$P_{6,6,6,14}$][DCA]), data for alcohol activity coefficients at infinite dilution are not available in the literature. Therefore, pure-IL density and solubility data of a reference sugar in the ILs were used for the parameter estimation. The reference sugar chosen was xylitol, which presents roughly an average value for the experimental solubility among the four solutes considered (see Tables 6 and 7 or Figure 8 in section 4 of this manuscript). Preliminary tests using this fitting strategy showed that the association

scheme for ILs should be the same as for the reference solute. Thus, the association scheme 5+5 was chosen for the ILs parameterized with this approach. As done for strategy 1, the association parameters of the ILs were set to the same constant values (ε^{AiBi}/k_B = 5000 K and κ^{AiBi} = 0.1). In strategy 2, a k_{ij} between the ILs and xylitol was considered as an additional adjustable parameter; however assumed to be temperature independent values. As a result, four adjustable parameters were fitted to pure-IL density and xylitol solubilities: m_i^{seg}, σ_i, u_i/k_B, and a k_{ij} between xylitol and IL. Table 3 lists the pure-IL and k_{ij} parameters obtained with this strategy 2.

Afterwards, and independently on the fitting strategy used, a k_{ij} for each binary system (sugar+IL) was applied to accurately describe the experimental solubility in ILs. They are listed in Table 4 for each parameter-estimation strategy. It can be observed that the absolute k_{ij} values are very low for strategy 1 and distinctly higher (one order of magnitude) for strategy 2. This already shows that it is highly recommended to use non-solubility related data for the IL-parameter estimation in order to obtain k_{ij} values that are as low (absolute) as possible.

4. Results and discussion

4.1. Experimental pure-IL densities

The densities of the pure ILs measured in this work are presented in Table 5 as a function of temperature. Figures 2 and 3 compare the data measured in this work with other data from open literature.

It can be observed from Figures 2 and 3 that our measured density data are in excellent agreement with literature data. An exception was found for Aliquat®[DCA] for which lower densities were obtained compared with literature data. This is probably due to the different amount of water in the IL. The Aliquat®[DCA] used in this work contained 0.05 wt% of water, which is lower than that present in the literature work[79] (0.2 wt%) and might explain the density discrepancy shown in Figure 3.

The large alkyl chains present in the hydrophobic ILs (Aliquat®[DCA] and [$P_{6,6,6,14}$][DCA]) cause high system volumes and low densities, even lower than 1000 kg/m^3 in the whole temperature range (see Figure 3). Densities are slightly different between these

two hydrophobic ILs although the alkyl-chain volume is similar. [$P_{6,6,6,14}$][DCA] possesses a higher number of alkyl groups (larger alkyl chains), which at a first glance would let one assigning to it a lower density than for Aliquat®[DCA], due to a larger volume occupancy of [$P_{6,6,6,14}$][DCA]. However, the molar mass of the ions also influences the IL density [82]: heavy ions cause high mass-density ILs. Thus, as the phosphorous central atom is heavier than nitrogen, [$P_{6,6,6,14}$][DCA] is "heavier" than Aliquat®[DCA]. Among the considered hydrophilic imidazolium-based ILs, [bmim][DCA] has a lower mass density than [emim][DCA] due to the higher number of alkyl groups in the cation which causes higher volumes related to a higher flexibility/mobility of the $[bmim]^+$. [emim][TFA] presents higher mass density than [emim][DCA] caused by the much higher molar mass of its anion (roughly the double). Besides the anion molar mass effect, the anion-cation interaction (both coulombic and hydrogen bonding) plays also a role in yielding more or less densier IL-structures. Thus, the acetate-based anion $[TFA]^-$ due to its higher lewis basicity (ability to accept hydrogen bonds) compared with $[DCA]^-$ can interact more strongly with the $[emim]^+$ cation resulting in an IL with higher density.

4.2. Experimental sugar alcohol solubility in ILs

Tables 6 and 7 show the experimental data of sugar alcohol solubility in the five ILs considered in this work. The solubility is presented in molality units, i.e. moles of sugar alcohol per kg of pure IL. The standard deviation is related to the triplicate sampling, and the relative uncertainty is calculated according to the theory of uncertainty propagation.

The presence of water in these systems might be an important factor that influences solubility values. Thus, in Table 8 the weight-percent values of water in the ILs before and after all the solubility measurements are presented. It was found out within this work that there is no significant impact on solubility data for water wt% differences lower than 0.2 wt%. As it can be seen from Table 8, water wt% differences for the ILs was always below this value and therefore reliable solubility data was obtained. For some ILs, the natural water uptake during sampling procedures was

higher than for others (e.g. for Aliquat®[DCA] in Table 8), but the critical difference of 0.2 wt% was never exceeded.

The analysis of the measured solubility data (see Tables 6 and 7) provides several conclusions. First, the ability of these ILs to dissolve xylitol and sorbitol depends on both the cation and the anion nature. Due to their electron-donor properties[18,20] both anions considered in this work ($[TFA]^-$ and $[DCA]^-$) show high affinity for sugars and sugar alcohols (see also Figure 1). The high free-electron density allows for strong hydrogen bonding between the IL anions and the hydroxyl groups of the sugar alcohols. This leads to high xylitol and sorbitol solubilities in ILs containing these anions. Comparing both anions, $[TFA]^-$ might have a higher hydrophilicity as the sugar solubility is generally higher in [emim][TFA] than in [emim][DCA]. This is illustrated in Figure 4. In addition, the free electrons in $[TFA]^-$ are more accessible due to steric effects. Thus, a higher hydrophilicity, i.e. stronger interactions with sugar OH groups and steric advantages, yields higher solubilities in [TFA]-based ILs compared to [DCA]-based ILs.

Besides the anion influence, the hydrophilicity of the ILs considered in this work depends strongly on the cation character. The hydrophilic ILs under investigation contain imidazolium-based cations ([emim][DCA], [bmim][DCA], and [emim][TFA]), whereas the hydrophobic ILs used in this work are Aliquat®[DCA] and $[P_{6,6,6,14}]$[DCA]. An evident conclusion is that the hydrophilic ILs dissolve much more xylitol and sorbitol than the hydrophobic ones (see Tables 6 and 7). This might be due to the fact that the large alkyl chains of the $[Aliquat]^+$ and the $[P_{6,6,6,14}]^+$cations interact preferably with each other. This causes strong IL-IL interactions and only weak solute-IL interactions.

The effect of the alkyl chain length of the ILs on sugar alcohol solubilities can be analyzed in Figure 5. Investigating the solubility of xylitol and sorbitol in $[emim]^+$ and $[bmim]^+$-based ILs with the same anion (dicyanamide), it was observed that the presence of the two additional CH_2 groups in [bmim][DCA] reduces the solubility of xylitol and sorbitol by more than 30 % (related to molality). Among the two hydrophobic ILs (Aliquat®[DCA] and $[P_{6,6,6,14}]$[DCA]), the higher solubility values were found in the Aliquat IL. As the same effect was observed in a previous work for the

solubility of glucose and of fructose[26], it seems that ILs with ammonium-based cations are generally more suitable as solvents for sugar-like molecules than ILs with phosphonium-based cations. However, it is important to note that the $[P_{6,6,6,14}]^+$ cation has more alkyl (apolar) groups than the Aliquat$^+$ cation, which also affects solubility (as shown for the $[emim]^+$ and $[bmim]^+$ cations in Figure 5).

As xylitol and sorbitol have very similar chemical structures, their solubility behavior in the selected ILs could be expected to be identical. On the one hand, sorbitol has an additional OH group compared to xylitol, which causes more hydrogen bonds with the ILs. On the other hand, sorbitol has also one CH group more (less polarity) than xylitol which causes the opposite effect. These contrary effects could compensate each other and as consequence, one could expect the xylitol/IL and the sorbitol/IL interactions to be very similar. Nevertheless, experimental data indicate that xylitol is slightly more soluble than sorbitol. This can probably be attributed to the different melting properties (Table 1), which are more favorable for xylitol solubility. However, sorbitol is more soluble than xylitol in [emim][DCA] and [bmim][DCA] until ca. 320 K (Figure 5). This might be due to higher hydrogen-bond strength at lower temperatures, causing the sugar with more OH groups (sorbitol) to be slightly more soluble. In addition, the melting-properties effect is not that significant at these lower temperatures, and a small increase in hydrogen bonding strength can reverse the solubility ranking.

Comparison between solubility data obtained in this work with those published by Paduszyński et al.[24] was performed. It should be noted that the experimental techniques for the determination of the solubilities applied in both works were clearly distinct. Nevertheless, Figure 5 shows that there is a good agreement between the data measured in this work and those reported by Paduszyński et al.[24]

4.3. Pure-IL PC-SAFT parameters

All the PC-SAFT parameter sets for the ILs listed in Tables 2 and 3 allow for accurate pure-IL density modeling (ARD < 1 %) in the temperature range from 278 to 343 K (Figures 2 and 3). Considering Tables 2 and 3, it can be observed that pure-IL density calculations are in better agreement with experimental data using strategy 1 (parameters fitted to IL density and 1-propanol activity coefficients at infinite dilution)

instead of strategy 2 (parameters fitted to IL density and xylitol solubility). This is probably due to the fact that the parameters in strategy 1 were estimated using data only at $x_{IL} \approx 1$ (pure-IL densities and 1-propanol activity coefficients at infinite dilution) whereas data at much lower IL concentrations ($x_{IL}<<1$) were used in strategy 2. Nevertheless, the density ARD value in density calculated for [bmim][DCA] (0.16 %) is close to that obtained by Paduszyński et al.[24] (ARD=0.10 %), who fitted the parameters to density data and vapor-pressure data of the pure IL.

The physical meaning of the parameter sets was assessed by calculating the vapor pressure of pure ILs. The scarcely reported experimental vapor pressure[83] of ILs indicate that vapor pressure of ILs should be lower than 3 Pa at temperatures until 500 K (note that such high temperature is close to the decomposition temperature of some ILs). Applying the parameters determined in this work (Tables 2 and 3) all the IL parameter sets presented in this work yield vapor pressures below 0.1 Pa up to 600 K, which is sounding with the "non-volatility" of the ILs. It is worth to note that this was achieved without applying any direct constraint. The selection of high values for association parameters and the number of association sites played a crucial role herein, and acted as an indirect constraint to vapor pressure.

In order to further test the suitability of the pure-IL parameters to describe the physical properties of ILs, the parameters were used to predict osmotic-coefficient data in IL+water and IL+(1-butanol) mixtures. Figure 6 compares experimental and PC-SAFT modeled osmotic coefficients in these solutions. It can be seen that the parameters provide a satisfactory qualitative prediction of the osmotic-coefficient data. This result is independent of the strategy applied for the parameter-estimation procedure: Figure 6a presents a system with pure-IL parameters estimated with strategy 1, whereas Figure 6b presents a system with pure-IL parameters estimated by strategy 2. A good quantitative modeling was obtained by fitting a k_{ij} to experimental data with better accuracy for the system where IL parameters were fitted using strategy 1. Figure 6 shows that the pure-IL PC-SAFT parameters determined in this work allow calculating thermodynamic properties that were not used in the parameter-estimation procedure.

As the PC-SAFT parameters for the ILs are applicable to different systems, different conditions, and various thermodynamic properties, they are proven to be physically meaningful and allow for a qualitative analysis. Since the association parameters were kept constant for all ILs used, the IL dispersion-energy parameter might be related with the solubility of the sugars in the ILs. In Tables 2 and 3 it can be observed that the higher the u_{IL}/k_B values, the higher the xylitol and sorbitol solubilities in the respective IL (data in Tables 6 and 7). This dependence holds for both, strategy 1 and 2.

A linear relation between ($m_{IL}^{seg}\cdot\sigma_{IL}^{3}\cdot M_{IL}^{-1}$) and the specific volume at 298 K was identified for the IL parameters determined by both strategies, which is illustrated by the circles in Figure 7a. A more complete IL database would allow for a better linear regression, which could be useful to decrease the number of adjustable parameters for other ILs with less data available. However, ILs with parameters obtained with strategy 2 (triangles in Figure 7a) produced some dispersion in the linear trend, which might be due to the fact that this strategy was applied without using data which accounts for IL-interactions at $x_{IL}\approx 1$. Nevertheless, strategy 2 IL parameters ($m_{IL}^{seg}\cdot\sigma_{IL}^{3}$ and u_{IL}/k_B) depend linearly on the IL molecular weight (see triangles in Figure 7b and 7c), which indicates that these parameters are also physically reasonable as similar relations were observed in many PC-SAFT modeling studies. These trends were not observed for strategy 1 (circles in Figure 7b and 7c) due to the very narrow range of molecular weights of the ILs used in that approach.

4.4. Modeling sugar and sugar alcohol solubility in ILs

The IL parameters obtained with strategy 1 (using pure-IL density and γ_{1-p}^{∞} data) were applied to directly predict the solubility of glucose, fructose, xylitol, and sorbitol in these ILs. That is, k_{ij} values between sugar and IL were set to zero. Figure 8 illustrates that solubilities are predicted reasonably well, with ARDs for glucose varying between 3.4 - 14.4, for xylitol between 15.5 - 34.9 %, and for sorbitol between 8.3 - 13.8 %. The ranking of solubility of the four sugars in all the ILs above 300 K is predicted correctly. Noteworthy, these predictions were performed using only three adjustable pure-IL parameters. The worst results were obtained for fructose, for which PC-SAFT

overpredicts the solubility in the three ILs considered leading to ARDs of 31.3, 33.7, and 112.2% for [emim][$EtSO_4$][22] [emim][DCA], and [emim][TFA], respectively. For xylitol in [emim][TFA], the solubility at 300 K is modeled in accordance to experimental data whereas the temperature dependence of the experimental solubility could not be correctly predicted. This might be due to the fact that temperature-independent Δc_p^{S-L} values were used for the modeling with Eq.(11), which might require applying temperature-dependent k_{ij} values.

Nevertheless, these predictions are quite satisfactory considering the fact that usually non-zero k_{ij} values are expected for the modeling of complex binary mixtures with PC-SAFT.

For the quantitative modeling of sugar solubility in ILs, k_{ij} values between a sugar or sugar alcohol and an IL were fitted to solubility data. The remarkably low k_{ij} values in these systems (see Table 4) also confirm that the solubility predictions with PC-SAFT are already in a reasonable agreement with the experimental data. Despite the fact that fructose solubility predictions were not as good as for the other solutes, quite satisfactory modeling results were obtained when k_{ij} values were implemented (Figure 9). Thus, Introducing k_{ij} parameters improves the solubility descriptions (maximum ARDs of 3.8, 5.3, and 10.9% for glucose, fructose, and sorbitol solubility, respectively) (see Table 9). For xylitol the maximum ARDs was 21.7%, obtained for solubility in [emim][TFA], due to the reasons explained above. However, for [emim][$EtSO_4$] and [emim][DCA] the ARDs were 7.0% and 10.8%, respectively.

The xylitol solubility fittings with IL-parameters obtained using strategy 2 are presented in Figure 10 (solid lines) and compared to the experimental data (squares in Figure 10). The experimental solubility data of xylitol shown in Figure 10 strongly depends on the kind of IL. Whereas the solubility of xylitol is relatively high in [bmim][DCA], it is extremely low in Aliquat®[DCA] and [$P_{6,6,6,14}$][DCA] even at elevated temperatures. With the Fitting of small k_{ij} values between xylitol and each IL (see Table 3), PC-SAFT is able to describe these solubility differences with good accuracy. The parameters yield very satisfactorily *ARD* values of 1.6, 6.9, and 11.2 % for [bmim][DCA], Aliquat®[DCA], and [$P_{6,6,6,14}$][DCA], respectively.

In Figure 10, the modeling results of glucose, fructose, and sorbitol solubility in ILs (using IL parameters obtained with strategy 2) are presented. Overall, the results are quite satisfactory, yielding ARDs (see also Table 10) in the range of 4.9 - 10.6% for glucose, 5.3 - 25.8% for fructose, and 5.4 - 17.3% for sorbitol. However, the steep increase of the fructose solubility in [$P_{6,6,6,14}$][DCA] in the temperature range from 318 to 328 K could not be quantitatively reproduced with PC-SAFT. This increase differs from the temperature dependence of the solubility behavior in all other systems. As the IL parameters were fitted to xylitol solubility where this unusual steep increase does not occur it might be assumed that the parameters are not appropriate to describe the extreme increase in fructose solubility at T > 318 K accurately.

Among the ILs parameterized with strategy 2, [bmim][DCA] has already been modeled by *Paduszyński et al.*[24] who used PC-SAFT to model the solubility of sugar alcohols over a wide temperature range (up to the melting temperature). However, in this work the solubility data were measured and modeled in a narrower temperature range. It is worth to assess how this model results can be extrapolated to higher temperatures. Thus, in Figure 11 the typical patterns of SLE diagrams calculated in this work are presented.

Figure 11 illustrates the application of PC-SAFT to the modeling of xylitol in [bmim][DCA] over a broad temperature range. The k_{ij} value between xylitol and [bmim][DCA] was adjusted in this work to solubility data in the temperature range between 290 and 330 K. Nevertheless, this k_{ij} can be applied also to extrapolate the solubility of xylitol up to the melting temperature of xylitol satisfactorily. Using PC-SAFT between 330 and 360 K yields only slightly higher xylitol solubilities than the experimental data of Paduszyński et al.[24]. In that work, the authors observed instabilities in the calculated SLE curve at high temperatures using the predictive form of PC-SAFT(k_{ij}=0). In this work the predictions (k_{ij}=0) do not present any instability region when calculating solubilities close to melting temperature for systems with [bmim][DCA]. This behavior was similar in the systems with the ILs [emim][EtSO4], [emim][DCA] and [emim][TFA], independent of the considered sugar or sugar alcohol. For all these ILs, PC-SAFT either predict well the solubilities or overpredict them (in the case of [bmim][DCA]). However, for the two ILs [$P_{6,6,6,14}$][DCA] and Aliquat®[DCA] instabilities were observed, similar to those reported by Paduszyński et al.[24].

Furthermore, liquid split phase was calculated in these two systems: [$P_{6,6,6,14}$][DCA] + xylitol and Aliquat®[DCA] + xylitol. Comparing the pure-component parameters of the ILs (see Table 3) and also those from Paduszyński et al. such instabilities might be due to too low values of u_i/k_B.

5. Conclusions

In this work, pure-IL density and solubility of sugars and sugar alcohols in ILs were investigated experimentally as well as modeled with PC-SAFT. Two sugars (glucose and fructose), two sugar alcohols (xylitol and sorbitol) and six ILs ([emim][DCA], [bmim][DCA], Aliquat[DCA], [$P_{6,6,6,14}$][DCA], [emim][ETSO4], and [emim][TFA]) were considered.

Measured pure-IL densities are in very good agreement with available literature data. Considering ILs with the same cation, the pure-IL densities were found to be generally higher for bigger anions. For ILs with the same anion, such a general trend could not be observed: On the one hand, pure densities of hydrophilic ILs ([emim][DCA] and [bmim][DCA]) were high for an IL with a short cation alkyl chain length. On the other hand, in hydrophobic ILs (Aliquat®[DCA] and [$P_{6,6,6,14}$][DCA]) high densities were found for the IL with a long cation alkyl chain length.

The measured solubility data of xylitol and sorbitol is in good agreement with literature data for [bmim][DCA]. The solubility data of these sugar alcohols in the other five ILs were presented for the first time and followed the trends found in our previous works for solubility of glucose and fructose in the same ILs. ILs with the $[TFA]^-$ anion have higher ability to dissolve the sugar alcohols than $[DCA]^-$-based ILs. The effect of the IL alkyl chain length on sugar alcohol solubility in these ILs revealed that increasing the alkyl chain length causes a strong decrease of solubilities. Among the hydrophobic ILs, the ammonium-based Aliquat®[DCA] dissolves higher amounts of xylitol and sorbitol than the phosphonium-based IL [$P_{6,6,6,14}$][DCA]. In general, xylitol was found to be more soluble than sorbitol, which might be explained by the more favorable

melting properties of xylitol. However, an exception was found in hydrophilic [DCA]-based ILs at low temperatures, in which sorbitol is more soluble than xylitol.

PC-SAFT pure-IL parameters were fitted for six ILs using two different strategies. In both strategies the pure-IL density was used to fit the parameters. In strategy 1, additionally 1-propanol infinite dilution activity coefficients, γ_{1-p}^{∞} (taken from literature) were used. In strategy 2 instead, xylitol solubility data in ILs were used for the parameter estimation together with the pure-density data. Comparing both strategies, slightly better pure IL-density descriptions were obtained with strategy 1. Further, sugar solubility in ILs could be predicted with a reasonable accuracy (ARDs < 30% in most cases) with strategy 1, i.e. without any knowledge of solubility data and k_{ij} = 0 between sugar and IL. The modeling results for systems with [bmim][DCA] were compared with those presented by Paduszyński et al.[24] (who first modeled SLE of sugar alcohols in ILs using PC-SAFT) showed overall good agreement and satisfactory results.

In sum, this work shows that PC-SAFT allows for quantitative modeling of the solubility of sugars in ILs, with only three pure-IL parameters. Further, this work has shown that accounting for association is crucial to model ILs. However, the association parameters do not need to be treated as adjustable parameters. Considering the obtained results, this work recommends fitting three pure-IL parameters to IL densities and infinite-dilution activity coefficients whenever available (strategy 1). In case of non-available experimental γ_1^{∞} data, the parameters can also be adjusted to solubility data of solutes in ILs (strategy 2 in this work). This requires three pure-IL parameters and a k_{ij} and allows only for the correlation of solubility data.

6. Acknowledgements

This work is partially supported by project PEst-C/EQB/LA0020/2011, financed by FEDER through COMPETE - Programa Operacional Factores de Competitividade and by FCT - Fundação para a Ciência e a Tecnologia. A.C. acknowledges financial support (Grant SFRH/BD/62105/2009) from Fundação para a Ciência e a Tecnologia (FCT, Portugal).

7. Nomenclature

Roman symbols

a	$J \cdot mol^{-1}$	molar Helmholtz free energy
k_B	$J \cdot K^{-1}$	Boltzmann constant, $1.38065 \cdot 10^{-23}$ $J \cdot K^{-1}$
k_{ij}		binary interaction parameter
m_i^{seg}		segment number
m_2	$mol \cdot kg^{-1}$	molality (moles of component 2 per kg of pure component 1)
M	$g \cdot mol^{-1}$	molar mass
N^{sites}		number of association sites
p	bar	pressure
R	$J \cdot mol^{-1} \cdot K^{-1}$	ideal gas constant, 8.314 $J \cdot mol^{-1} \cdot K^{-1}$
m	$mol \cdot kg^{-1}$	solubility of a sugar in IL (moles of sugar per kg of pure IL)
T	K	temperature
T_{0i}^{S-L}	K	melting temperature of pure component i
u_i/k_B	K	dispersion-energy parameter
u		uncertainty
wt%		weight fraction
x_i		mole fraction
Z		compressibility factor

Greek symbols

γ_1^{∞}		activity coefficient at infinite dilution of compound 1 in component 2
$\Delta c_{p,i}^{S-L}$	$J \cdot mol^{-1} \cdot K^{-1}$	Heat capacity difference between solid and liquid sugar
ΔH_{0i}^{S-L}	$J \cdot mol^{-1}$	melting enthalpy of pure component i
ε^{AiBi}/k_B	K	association-energy parameter
κ^{AiB}		association-volume parameter
ρ	$kg \cdot m^{-3}$	density
σ_i	Å	segment diameter
φ_i		fugacity coefficient
ϕ		osmotic coefficient

Subscripts

i, j	component indexes
S-L	solid-liquid
0	pure component
1	volatile component
2	non-volatile component
1-p	1-propanol
∞	infinite dilution

Superscripts

assoc	association
disp	dispersion
hc	hard chain
res	residual

Abbreviations

ARD	average relative deviation
EoS	equation of state
ILs	ionic liquids
OF	objective function
PC-SAFT	Perturbed-chain statistical-associating fluid theory
$[BF_4]^-$	tetrafluoroborate anion
$[emim]^+$	1-ethyl-3-methylimidazolium cation
$[bmim]^+$	1-butyl-3-methylimidazolium cation
$[DCA]^-$	dicyanamide anion
$[NTf_2]^-$	bis(trifluoromethylsulfonyl)imide anion
$[P_{6,6,6,14}]^+$	trihexyltetradecylphosphonium cation
$[PF_6]^-$	hexafluorophosphate anion
$[TFA]^-$	trifluoroacetate

8. References

(1) Werpy, T. A.; Petersen, G. *Top Value Added Chemicals From Biomass: I. Results of Screening for Potential Candidates from Sugars and Synthesis Gas*, Pacific Northwest National Laboratory, 2004.

(2) Plechkova, N. V.; Seddon, K. R. Applications of ionic liquids in the chemical industry *Chem. Soc. Rev.* **2008**, *37*, 123-150.

(3) Zhao, H.; Xia, S. Q.; Ma, P. S. Use of ionic liquids as 'green' solvents for extractions *J. Chem. Technol. Biotechnol.* **2005**, *80*, 1089-1096.

(4) Zhao, D. B.; Wu, M.; Kou, Y.; Min, E. Ionic liquids: applications in catalysis *Catal. Today* **2002**, *74*, 157-189.

(5) Welton, T. Room-temperature ionic liquids. Solvents for synthesis and catalysis *Chem. Rev.* **1999**, *99*, 2071-2083.

(6) Brennecke, J. F.; Maginn, E. J. Ionic liquids: Innovative fluids for chemical processing *AIChE J.* **2001**, *47*, 2384-2389.

(7) Huddleston, J. G.; Willauer, H. D.; Swatloski, R. P.; Visser, A. E.; Rogers, R. D. Room temperature ionic liquids as novel media for 'clean' liquid-liquid extraction *Chem. Commun.* **1998**, 1765-1766.

(8) Tan, S. S. Y.; MacFarlane, D. R. Ionic Liquids in Biomass Processing *Top. Curr. Chem.* **2009**, *290*, 311-339.

(9) da Costa Lopes, A.; João, K.; Morais, A.; Bogel-Łukasik, E.; Bogel-Łukasik, R. Ionic liquids as a tool for lignocellulosic biomass fractionation *sustain chem process* **2013**, *1*, 1-31.

(10) Sun, N.; Rodriguez, H.; Rahman, M.; Rogers, R. D. Where are ionic liquid strategies most suited in the pursuit of chemicals and energy from lignocellulosic biomass? *Chem. Commun.* **2011**, *47*, 1405-1421.

(11) da Costa Lopes, A. M.; João, K. G.; Rubik, D. F.; Bogel-Łukasik, E.; Duarte, L. C.; Andreaus, J.; Bogel-Łukasik, R. Pre-treatment of lignocellulosic biomass using ionic liquids: Wheat straw fractionation *Bioresour. Technol.* **2013**, *142*, 198-208.

(12) Long, J.; Li, X.; Guo, B.; Wang, L.; Zhang, N. Catalytic delignification of sugarcane bagasse in the presence of acidic ionic liquids *Catal. Today* **2013**, *200*, 99-105.

(13) Shill, K.; Padmanabhan, S.; Xin, Q.; Prausnitz, J. M.; Clark, D. S.; Blanch, H. W. Ionic Liquid Pretreatment of Cellulosic Biomass: Enzymatic Hydrolysis and Ionic Liquid Recycle *Biotechnol. Bioeng.* **2011**, *108*, 511-520.

(14) Iguchi, M.; Aida, T. M.; Watanabe, M.; Smith, R. L. Dissolution and recovery of cellulose from 1-butyl-3-methylimidazolium chloride in presence of water *Carbohydr. Polym.* **2013**, *92*, 651-658.

(15) Moreau, C.; Finiels, A.; Vanoye, L. Dehydration of fructose and sucrose into 5-hydroxymethylfurfural in the presence of 1-H-3-methyl imidazolium chloride acting both as solvent and catalyst *J Mol Catal a-Chem* **2006**, *253*, 165-169.

(16) Forsyth, S. A.; MacFarlane, D. R.; Thomson, R. J.; von Itzstein, M. Rapid, clean, and mild O-acetylation of alcohols and carbohydrates in an ionic liquid *Chem. Commun.* **2002**, 714-715.

(17) Forsyth, S. A.; MacFarlane, D. R. 1-alkyl-3-methylbenzotriazolium salts: ionic solvents and electrolytes *J. Mater. Chem.* **2003**, *13*, 2451-2456.

(18) Liu, Q.; Janssen, M. H. A.; van Rantwijk, F.; Sheldon, R. A. Room-temperature ionic liquids that dissolve carbohydrates in high concentrations *Green Chem.* **2005**, *7*, 39.

(19) Lee, S. H.; Dang, D. T.; Ha, S. H.; Chang, W.-J.; Koo, Y.-M. Lipase-catalyzed synthesis of fatty acid sugar ester using extremely supersaturated sugar solution in ionic liquids *Biotechnol. Bioeng.* **2008**, *99*, 1-8.

(20) Zhao, H.; Baker, G. A.; Song, Z.; Olubajo, O.; Crittle, T.; Peters, D. Designing enzyme-compatible ionic liquids that can dissolve carbohydrates *Green Chem.* **2008**, *10*, 696.

(21) Rosatella, A. A.; Branco, L. C.; Afonso, C. A. M. Studies on dissolution of carbohydrates in ionic liquids and extraction from aqueous phase *Green Chem.* **2009**, *11*, 1406-1413.

(22) Carneiro, A. P.; Rodriguez, O.; Macedo, E. A. Solubility of monosaccharides in ionic liquids - Experimental data and modeling *Fluid Phase Equilib.* **2012**, *314*, 22-28.

(23) Conceiçao, L. J. A.; Bogel-Lukasik, E.; Bogel-Lukasik, R. A new outlook on solubility of carbohydrates and sugar alcohols in ionic liquids *Rsc Adv* **2012**, *2*, 1846-1855.

(24) Paduszyński, K.; Okuniewski, M.; Domańska, U. Renewable Feedstocks in Green Solvents: Thermodynamic Study on Phase Diagrams of d-Sorbitol and Xylitol with Dicyanamide Based Ionic Liquids *The Journal of Physical Chemistry B* **2013**, *117*, 7034-7046.

(25) Carneiro, A. P.; Rodriguez, O.; Macedo, E. A. Solubility of xylitol and sorbitol in ionic liquids - Experimental data and modeling *J. Chem. Thermodyn.* **2012**, *55*, 184-192.

(26) Carneiro, A. P.; Rodríguez, O.; Macedo, E. A. Fructose and Glucose Dissolution in Ionic Liquids: Solubility and Thermodynamic Modeling *Ind. Eng. Chem. Res.* **2013**.

(27) Payne, S. M.; Kerton, F. M. Solubility of bio-sourced feedstocks in 'green' solvents *Green Chem.* **2010**, *12*, 1648-1653.

(28) Zakrzewska, M. E.; Bogel-Lukasik, E.; Bogel-Lukasik, R. Solubility of Carbohydrates in Ionic Liquids *Energ. Fuel.* **2010**, *24*, 737-745.

(29) Renon, H.; Prausnitz, J. M. Local compositions in thermodynamic excess functions for liquid mixtures *AIChE J.* **1968**, *14*, 135-144.

(30) Abrams, D. S.; Prausnitz, J. M. Statistical Thermodynamics of Liquid-Mixtures - New Expression for Excess Gibbs Energy of Partly or Completely Miscible Systems *AIChE J.* **1975**, *21*, 116-128.

(31) Feng, W.; Vanderkooi, H.; Deswaanarons, J. Application of the SAFT equation of state to biomass fast pyrolysis liquid *Chem. Eng. Sci.* **2005**, *60*, 617-624.

(32) Huang, S. H.; Radosz, M. Equation of State for Small, Large, Polydisperse, and Associating Molecules *Ind. Eng. Chem. Res.* **1990**, *29*, 2284-2294.

(33) Ji, P. J.; Feng, W.; Tan, T. W. Density calculation of sugar solutions with the SAFT model *J. Chem. Eng. Data* **2007**, *52*, 135-140.

(34) Ji, P. J.; Feng, W.; Tan, T. W.; Zheng, D. X. Modeling of water activity, oxygen solubility and density of sugar and sugar alcohol solutions *Food Chem.* **2007**, *104*, 551-558.

(35) Held, C.; Carneiro, A. P.; Rodríguez, O.; Sadowski, G.; Macedo, E. A. Modeling thermodynamic properties of aqueous single-solute and multi-solute sugar solutions with PC-SAFT *AIChE J.* **2013**. DOI: 10.1002/aic.14212

(36) Maia, F. M.; Tsivintzelis, I.; Rodriguez, O.; Macedo, E. A.; Kontogeorgis, G. M. Equation of state modelling of systems with ionic liquids: Literature review and application with the Cubic Plus Association (CPA) model *Fluid Phase Equilib.* **2012**, *332*, 128-143.

(37) Vega, L. F.; Vilaseca, O.; Llovell, F.; Andreu, J. S. Modeling ionic liquids and the solubility of gases in them: Recent advances and perspectives *Fluid Phase Equilib.* **2010**, *294*, 15-30.

(38) Kroon, M. C.; Karakatsani, E. K.; Economou, I. G.; Witkamp, G. J.; Peters, C. J. Modeling of the carbon dioxide solubility in imidazolium-based ionic liquids with the tPC-PSAFT equation of state *J. Phys. Chem. B* **2006**, *110*, 9262-9269.

(39) Nann, A.; Mündges, J.; Held, C.; Verevkin, S. P.; Sadowski, G. Molecular Interactions in 1-Butanol + IL Solutions by Measuring and Modeling Activity Coefficients *The Journal of Physical Chemistry B* **2013**, *117*, 3173-3185.

(40) Dománska, U.; Zawadzki, M.; Paduszynski, K.; Krolikowski, M. Perturbed-Chain SAFT as a Versatile Tool for Thermodynamic Modeling of Binary Mixtures Containing Isoquinolinium Ionic Liquids *J. Phys. Chem. B* **2012**, *116*, 8191-8200.

(41) Chen, Y. S.; Mutelet, F.; Jaubert, J. N. Modeling the Solubility of Carbon Dioxide in Imidazolium-Based Ionic Liquids with the PC-SAFT Equation of State *J. Phys. Chem. B* **2012**, *116*, 14375-14388.

(42) Andreu, J. S.; Vega, L. F. Capturing the solubility Behavior of CO2 in ionic liquids by a simple model *J. Phys. Chem. C* **2007**, *111*, 16028-16034.

(43) Ashrafmansouri, S. S.; Raeissi, S. Modeling gas solubility in ionic liquids with the SAFT-gamma group contribution method *J. Supercrit. Fluids* **2012**, *63*, 81-91.

(44) Rahmati-Rostami, M.; Behzadi, B.; Ghotbi, C. Thermodynamic modeling of hydrogen sulfide solubility in ionic liquids using modified SAFT-VR and PC-SAFT equations of state *Fluid Phase Equilib.* **2011**, *309*, 179-189.

(45) Ji, X.; Adidharma, H. Thermodynamic modeling of ionic liquid density with heterosegmented statistical associating fluid theory *Chem. Eng. Sci.* **2009**, *64*, 1985-1992.

(46) Ji, X.; Held, C.; Sadowski, G. Modeling imidazolium-based ionic liquids with ePC-SAFT *Fluid Phase Equilib.* **2012**, *335*, 64-73.

(47) Paduszyński, K.; Domańska, U. Solubility of Aliphatic Hydrocarbons in Piperidinium Ionic Liquids: Measurements and Modeling in Terms of Perturbed-Chain Statistical Associating Fluid Theory and Nonrandom Hydrogen-Bonding Theory *The Journal of Physical Chemistry B* **2011**, *115*, 12537-12548.

(48) Gross, J.; Sadowski, G. Perturbed-chain SAFT: An equation of state based on a perturbation theory for chain molecules *Ind. Eng. Chem. Res.* **2001**, *40*, 1244-1260.

(49) Shi, C.; Ge, Q.; Zhou, F.; Cai, M.; Wang, X.; Fang, X.; Pan, X. An improved preparation of 3-ethyl-1-methylimidazolium trifluoroacetate and its application in dye sensitized solar cells *Solar Energy* **2009**, *83*, 108-112.

(50) Kulkarni, P. S.; Branco, L. C.; Crespo, J. G.; Nunes, M. C.; Raymundo, A.; Afonso, C. A. M. Comparison of Physicochemical Properties of New Ionic Liquids Based on Imidazolium, Quaternary Ammonium, and Guanidinium Cations *Chemistry - A European Journal* **2007**, *13*, 8478-8488.

(51) Llovell, F.; Valente, E.; Vilaseca, O.; Vega, L. F. Modeling Complex Associating Mixtures with [C-n-mim][Tf2N] Ionic Liquids: Predictions from the Soft-SAFT Equation *J. Phys. Chem. B* **2011**, *115*, 4387-4398.

(52) Youngs, T. G. A.; Holbrey, J. D.; Mullan, C. L.; Norman, S. E.; Lagunas, M. C.; D'Agostino, C.; Mantle, M. D.; Gladden, L. F.; Bowron, D. T.; Hardacre, C. Neutron diffraction, NMR and molecular dynamics study of glucose dissolved in the ionic liquid 1-ethyl-3-methylimidazolium acetate *Chemical Science* **2011**, *2*, 1594-1605.

(53) Remsing, R. C.; Hernandez, G.; Swatloski, R. P.; Massefski, W. W.; Rogers, R. D.; Moyna, G. Solvation of carbohydrates in N,N '-dialkylimidazolium ionic liquids: A multinuclear NMR spectroscopy study *J. Phys. Chem. B* **2008**, *112*, 11071-11078.

(54) Wolbach, J. P.; Sandler, S. I. Using molecular orbital calculations to describe the phase behavior of cross-associating mixtures *Ind. Eng. Chem. Res.* **1998**, *37*, 2917-2928.

(55) Prausnitz, J. M.; Lichtenthaler, R. N.; Azevedo, E. G. *Molecular Thermodynamics of Fluid-Phase Equilibria* third ed.; Prentice Hall: New Jersey, 1999.

(56) Raemy, A.; Schweizer, T. F. Thermal behaviour of carbohydrates studied by heat flow calorimetry *J. Therm. Anal.* **1983**, *28*, 95-108.

(57) Roos, Y. Melting and glass transitions of low molecular weight carbohydrates *Carbohydr. Res.* **1993**, *238*, 39-48.

(58) Ferreira, O.; Brignole, E. A.; Macedo, E. A. Phase equilibria in sugar solutions using the A-UNIFAC model *Industrial & Engineering Chemistry Research* **2003**, *42*, 6212-6222.

(59) Catté, M.; Dussap, C.-G.; Achard, C.; Gros, J.-B. Excess properties and solid-liquid equilibria for aqueous solutions of sugars using a UNIQUAC model *Fluid Phase Equilib.* **1994**, *96*, 33-50.

(60) Tong, B.; Tan, Z.-C.; Shi, Q.; Li, Y.-S.; Yue, D.-T.; Wang, S.-X. Thermodynamic investigation of several natural polyols (I): Heat capacities and thermodynamic properties of xylitol *Thermochim. Acta* **2007**, *457*, 20-26.

(61) Yaws, C. L. Yaws' Handbook of Thermodynamic and Physical Properties of Chemical Compounds, Knovel **2003**.

(62) Mota, F. L.; Queimada, A. J.; Pinho, S. P.; Macedo, E. A. Water solubility of drug-like molecules with the cubic-plus-association equation of state *Fluid Phase Equilib.* **2010**, *298*, 75-82.

(63) Calvar, N.; Gomez, E.; Dominguez, A.; Macedo, E. A. Determination and modelling of osmotic coefficients and vapour pressures of binary systems 1-and 2-propanol with C(n)MimNTf(2) ionic liquids (n=2, 3, and 4) at T=323.15 K *J. Chem. Thermodyn.* **2011**, *43*, 1256-1262.

(64) Calvar, N.; Gomez, E.; Dominguez, A.; Macedo, E. A. Vapour pressures, osmotic and activity coefficients for binary mixtures containing (1-ethylpyridinium ethylsulfate plus several alcohols) at T=323.15 K *J. Chem. Thermodyn.* **2010**, *42*, 625-630.

(65) Calvar, N.; Gonzalez, B.; Dominguez, A.; Macedo, E. A. Osmotic coefficients of binary mixtures of 1-butyl-3-methylimidazolium methylsulfate and 1,3-dimethylimidazolium methylsulfate with alcohols at T=323.15 K *J. Chem. Thermodyn.* **2009**, *41*, 617-622.

(66) Gomez, E.; Gonzalez, B.; Calvar, N.; Tojo, E.; Dominguez, A. Physical properties of pure 1-ethyl-3-methylimidazolium ethylsulfate and its binary mixtures with ethanol and water at several temperatures *J. Chem. Eng. Data* **2006**, *51*, 2096-2102.

(67) Rodríguez, H.; Brennecke, J. F. Temperature and Composition Dependence of the Density and Viscosity of Binary Mixtures of Water + Ionic Liquid *J. Chem. Eng. Data* **2006**, *51*, 2145-2155.

(68) González, E. J.; González, B.; Calvar, N.; Domínguez, Á. Physical Properties of Binary Mixtures of the Ionic Liquid 1-Ethyl-3-methylimidazolium Ethyl Sulfate with Several Alcohols at T = (298.15, 313.15, and 328.15) K and Atmospheric Pressure *J. Chem. Eng. Data* **2007**, *52*, 1641-1648.

(69) Hofman, T.; Goldon, A.; Nevines, A.; Letcher, T. M. Densities, excess volumes, isobaric expansivity, and isothermal compressibility of the (1-ethyl-3-methylimidazolium ethylsulfate plus methanol) system at temperatures (283.15 to 333.15) K and pressures from (0.1 to 35) MPa *J. Chem. Thermodyn.* **2008**, *40*, 580-591.

(70) Wong, C. L.; Soriano, A. N.; Li, M. H. Diffusion coefficients and molar conductivities in aqueous solutions of 1-ethyl-3-methylimidazolium-based ionic liquids *Fluid Phase Equilib.* **2008**, *271*, 43-52.

(71) Sumartschenkowa, I. A.; Verevkin, S. P.; Vasiltsova, T. V.; Bich, E.; Heintz, A.; Shevelyova, M. P.; Kabo, G. J. Experimental Study of Thermodynamic Properties of Mixtures Containing Ionic Liquid 1-Ethyl-3-methylimidazolium Ethyl Sulfate Using Gas−Liquid Chromatography and Transpiration Method *J. Chem. Eng. Data* **2006**, *51*, 2138-2144.

(72) Quijada-Maldonado, E.; van der Boogaart, S.; Lijbers, J. H.; Meindersma, G. W.; de Haan, A. B. Experimental densities, dynamic viscosities and surface tensions of the ionic liquids series 1-ethyl-3-methylimidazolium acetate and dicyanamide and their binary and ternary mixtures with water and ethanol at T = (298.15 to 343.15 K) *J. Chem. Thermodyn.* **2012**, *51*, 51-58.

(73) Schreiner, C.; Zugmann, S.; Hartl, R.; Gores, H. J. Fractional Walden Rule for Ionic Liquids: Examples from Recent Measurements and a Critique of the So-Called Ideal KCl Line for the Walden Plot *J. Chem. Eng. Data* **2010**, *55*, 1784-1788.

(74) Mutelet, F.; Revelli, A. L.; Jaubert, J. N.; Sprunger, L. M.; Acree, W. E.; Baker, G. A. Partition Coefficients of Organic Compounds in New Imidazolium and Tetralkylammonium Based Ionic Liquids Using Inverse Gas Chromatography *J. Chem. Eng. Data* **2010**, *55*, 234-242.

(75) Dománska, U.; Marciniak, A. Activity coefficients at infinite dilution measurements for organic solutes and water in the ionic liquid 1-ethyl-3-methylimidazolium trifluoroacetate *J. Phys. Chem. B* **2007**, *111*, 11984-11988.

(76) Fredlake, C. P.; Crosthwaite, J. M.; Hert, D. G.; Aki, S. N. V. K.; Brennecke, J. F. Thermophysical Properties of Imidazolium-Based Ionic Liquids *J. Chem. Eng. Data* **2004**, *49*, 954-964.

(77) Sanchez, L. G.; Espel, J. R.; Onink, F.; Meindersma, G. W.; de Haan, A. B. Density, Viscosity, and Surface Tension of Synthesis Grade Imidazolium, Pyridinium, and Pyrrolidinium Based Room Temperature Ionic Liquids *J. Chem. Eng. Data* **2009**, *54*, 2803-2812.

(78) Carvalho, P. J.; Regueira, T.; Santos, L. M. N. B. F.; Fernandez, J.; Coutinho, J. A. P. Effect of Water on the Viscosities and Densities of 1-Butyl-3-methylimidazolium Dicyanamide and 1-Butyl-3-methylimidazolium Tricyanomethane at Atmospheric Pressure *J. Chem. Eng. Data* **2010**, *55*, 645-652.

(79) Nieto de Castro, C. A.; Langa, E.; Morais, A. L.; Lopes, M. L. M.; Lourenço, M. J. V.; Santos, F. J. V.; Santos, M. S. C. S.; Lopes, J. N. C.; Veiga, H. I. M.; Macatrão, M.; Esperança, J. M. S. S.; Marques, C. S.; Rebelo, L. P. N.; Afonso, C. A. M. Studies on the density, heat capacity, surface tension and infinite dilution diffusion with the ionic liquids [C4mim][NTf2], [C4mim][dca], [C2mim][EtOSO3] and [Aliquat][dca] *Fluid Phase Equilib.* **2010**, *294*, 157-179.

(80) Pereiro, A. B.; Veiga, H. I. M.; Esperanca, J. M. S. S.; Rodriguez, A. Effect of temperature on the physical properties of two ionic liquids *J. Chem. Thermodyn.* **2009**, *41*, 1419-1423.

(81) Rodriguez, H.; Brennecke, J. F. Temperature and composition dependence of the density and viscosity of binary mixtures of water plus ionic liquid *J. Chem. Eng. Data* **2006**, *51*, 2145-2155.

(82) Jacquemin, J.; Ge, R.; Nancarrow, P.; Rooney, D. W.; Gomes, M. F. C.; Padua, A. A. H.; Hardacre, C. Prediction of ionic liquid properties. I. Volumetric properties as a function of temperature at 0.1 MPa *J. Chem. Eng. Data* **2008**, *53*, 716-726.

(83) Emel'yanenko, V. N.; Verevkin, S. P.; Heintz, A. The gaseous enthalpy of formation of the ionic liquid 1-butyl-3-methylimidazolium dicyanamide from combustion calorimetry, vapor pressure measurements, and ab initio calculations *J. Am. Chem. Soc.* **2007**, *129*, 3930-3937.

(84) Calvar, N.; Gonzalez, B.; Dominguez, A.; Macedo, E. A. Osmotic coefficients of binary mixtures of four ionic liquids with ethanol or water at T = (313.15 and 333.15) K *J. Chem. Thermodyn.* **2009**, *41*, 11-16.

(85) Calvar, N.; Gonzalez, E. J.; Dominguez, A.; Macedo, E. A. Acoustic, volumetric and osmotic properties of binary mixtures containing the ionic liquid 1-butyl-3-methylimidazolium dicyanamide mixed with primary and secondary alcohols *J. Chem. Thermodyn.* **2012**, *50*, 19-29.

Figure Captions

Figure 1. Chemical structure of the ionic species present in the ionic liquids considered within this work

Figure 2. Density of [emim]$^+$-based ILs. Comparison between experimental data measured in this work (black symbols) and from literature (grey symbols): [emim][DCA] triangles [72], [emim][TFA] circles[81], and [emim][$EtSO_4$] squares (see refs. in Table 2). Lines are modeling results with PC-SAFT using the parameters from Table 2, obtained with strategy 1.

Figure 3. Density of [DCA]$^+$-based ILs. Comparison between experimental data measured in this work (black symbols) and from literature (grey symbols): [bmim][DCA] squares (refs. Table 3), Aliquat®[DCA] triangles[79], and [P6,6,6,14][DCA] circles[80]. Lines are modeling results with PC-SAFT using the parameters from Table 3, obtained with strategy 2.

Figure 4. Comparison of experimental solubility of glucose[26], fructose[26], xylitol, and sorbitol in [emim][TFA] (black bars) and in [emim][DCA] (grey bars) at 298 K.

Figure 5. Xylitol (squares) and sorbitol (triangles) solubility in [emim][DCA] (dark grey) and [bmim][DCA] (light grey) measured in this work. For comparison, data from the work of Paduszyński et al.[24] within the temperature range of the data measured in this work, are represented by unfilled symbols.

Figure 6. PC-SAFT predictions (dashed lines) and correlations (solid lines) with a) k_{ij}=-0.0088 and b) k_{ij}=0.022, and experimental data (squares) of osmotic coefficients in IL systems: a) water + [emim][$EtSO_4$] at 333.15 K [84] and b) 1-butanol + [bmim][DCA] at 323.15 K [85].

Figure 7. Relations between: a) ($m_{IL}^{seg}\cdot\sigma_{IL}^3\cdot M_{IL}^{-1}$) and specific volume at 298K, b) ($m_{IL}^{seg}\cdot\sigma_{IL}^3$) and molecular weight of ILs, c) u_i/k_B and molecular weight of ILs . Squares represent IL-parameters from Table 2 (strategy 1) and triangles the parameters from Table 3 (strategy 2).

Figure 8. Solubility of sugars in ILs versus temperature. Symbols are experimental data (circles: glucose[26], diamonds: fructose[26] , squares: xylitol, triangles: sorbitol) in: a)[emim][$EtSO_4$][22], b)[emim][DCA] and c)[emim][TFA]. Lines represent PC-SAFT predictions (dash-dot: glucose, long dash: fructose, solid line: xylitol, dotted: sorbitol) with parameters from Tables 1 and 2 (k_{ij}=0 between sugar and IL).

Figure 9. Solubility of fructose in ILs versus temperature. Symbols are experimental data (squares:[emim][EtSO4][22], triangles:[emim][DCA][26], circles:[emim][TFA][26]). Lines represent PC-SAFT correlations (solid line:[emim][EtSO4], dotted:[emim][DCA], dash-dot:[emim][TFA]) with parameters from Tables 1, 2, and 4.

Figure 10. Solubility of sugars and sugar alcohols in ILs: a)[bmim][DCA], b)Aliquat®[DCA] and c)[$P_{6,6,6,14}$][DCA] versus temperature. Symbols are experimental data: (circles: glucose[26] , diamonds: fructose [26], squares: xylitol, triangles: sorbitol), lines represent PC-SAFT correlations (dash-dot: glucose, long dash: fructose, solid line: xylitol, dotted: sorbitol) with parameters from Tables 1,3, and 4.

Figure 11. Solubility of xylitol in [bmim][DCA]. Solid line represents the PC-SAFT correlation with parameters from Tables 3 and 4. Dashed line is the PC-SAFT prediction (k_{ij}=0 between xylitol and [bmim][DCA]). Grey and black circles are experimental data from this work and from *Paduszyński et al*[24]., respectively. Inverted triangle represents the melting temperature of pure xylitol taken from literature (references from Table 1).

Figures

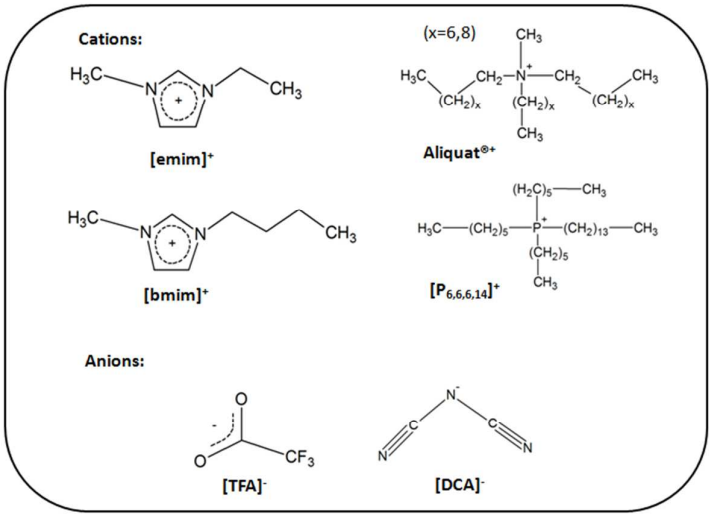

Figure 1

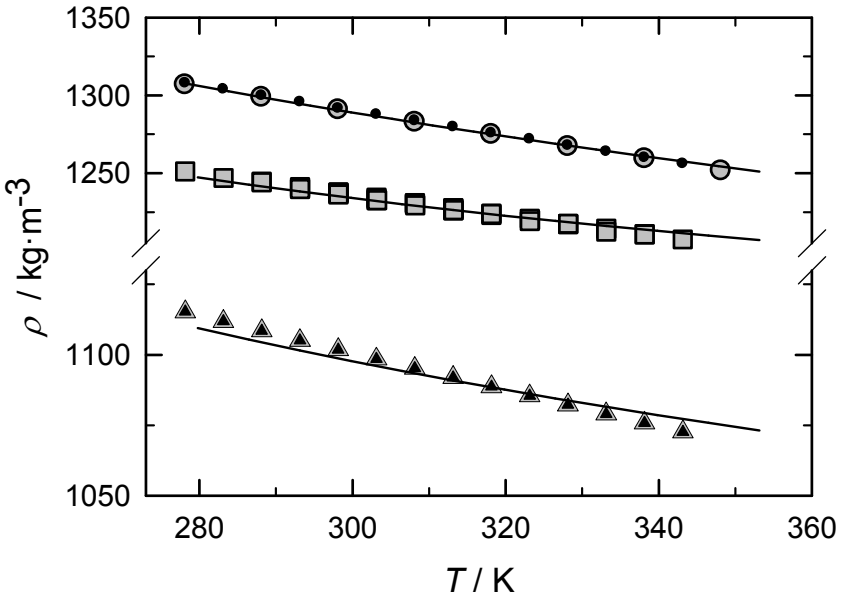

Figure 2

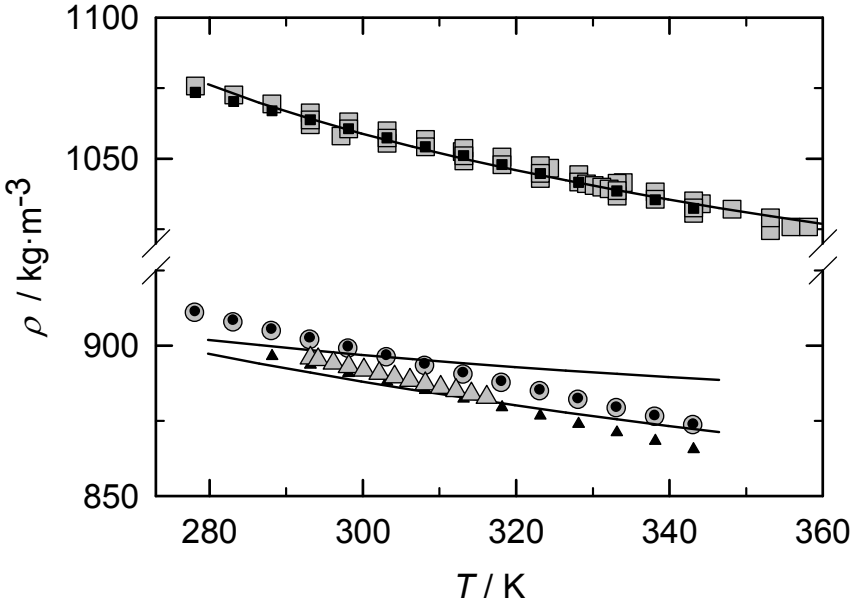

Figure 3

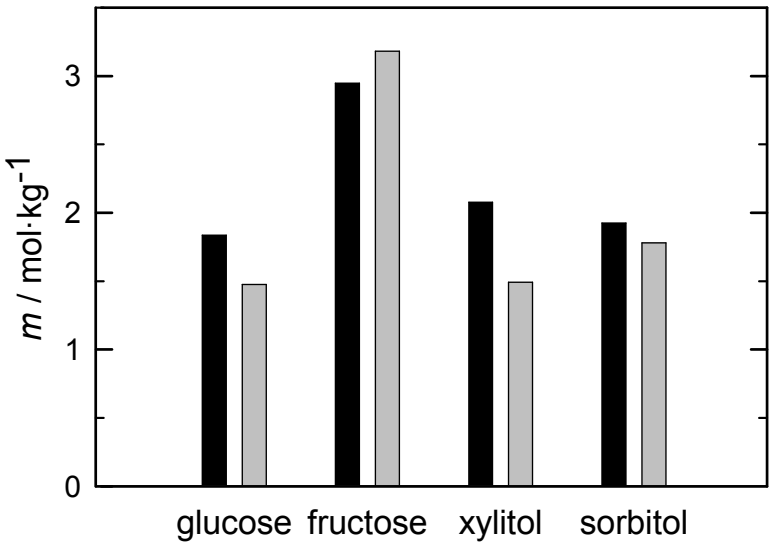

Figure 4

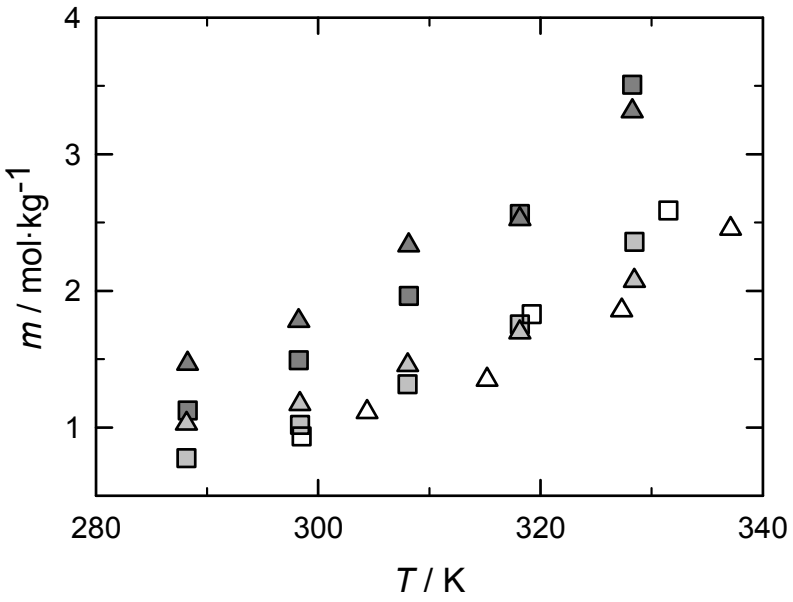

Figure 5

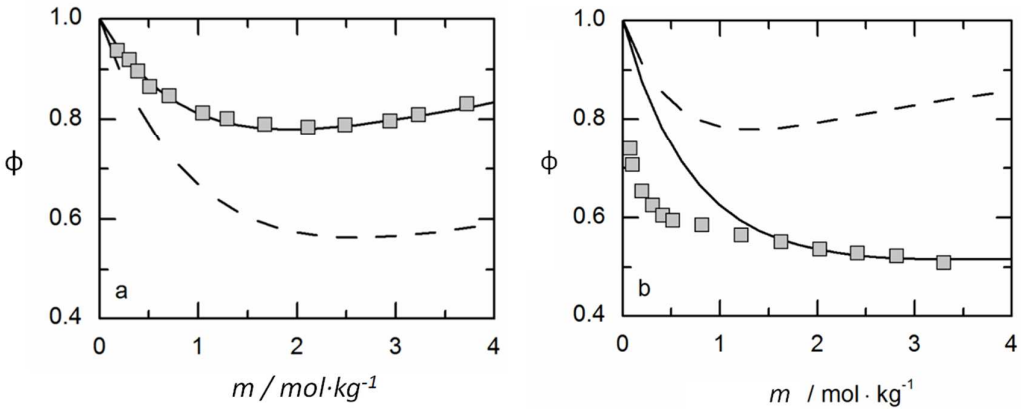

Figure 6

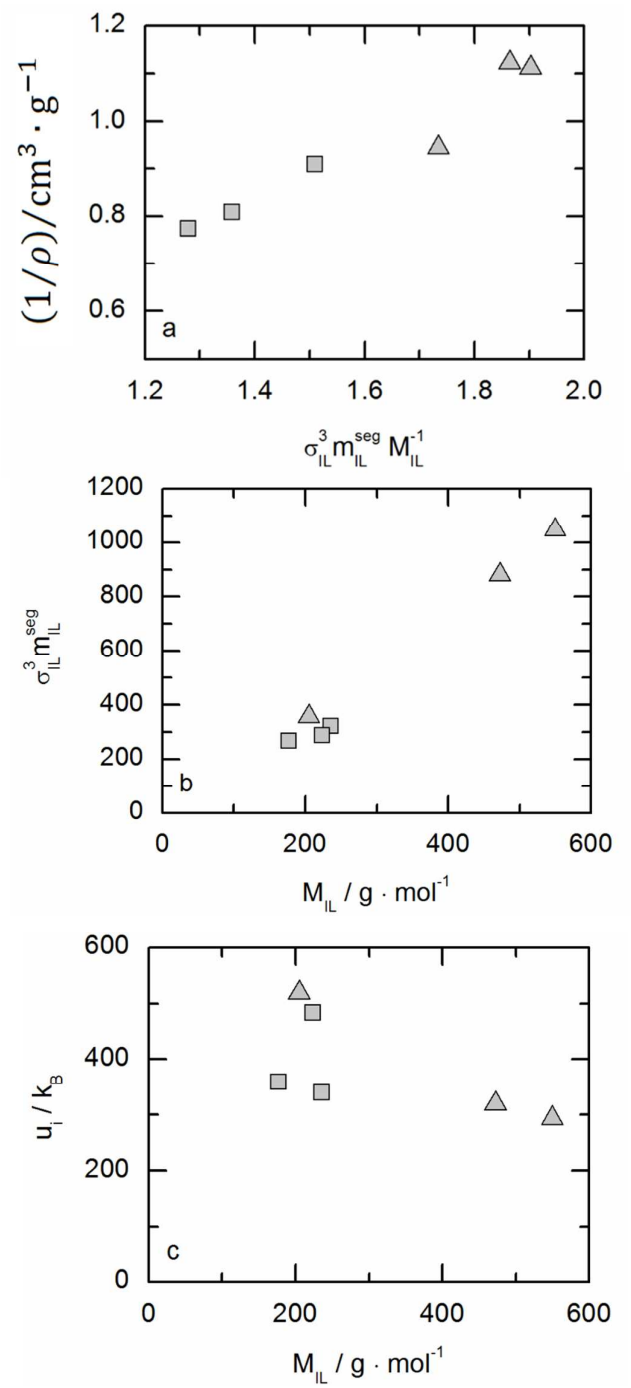
(1/ρ)/cm³ · g⁻¹
1.2
1.0
0.8
0.6
a
1.2
1.4
1.6
1.8
2.0
σ³IL mseg IL M-1 IL
σ³IL mseg IL
1200
1000
800
600
400
200
0
b
0
200
400
600
MIL / g · mol-1
ui / kB
600
400
200
0
c
0
200
400
600
MIL / g · mol-1

Figure 7

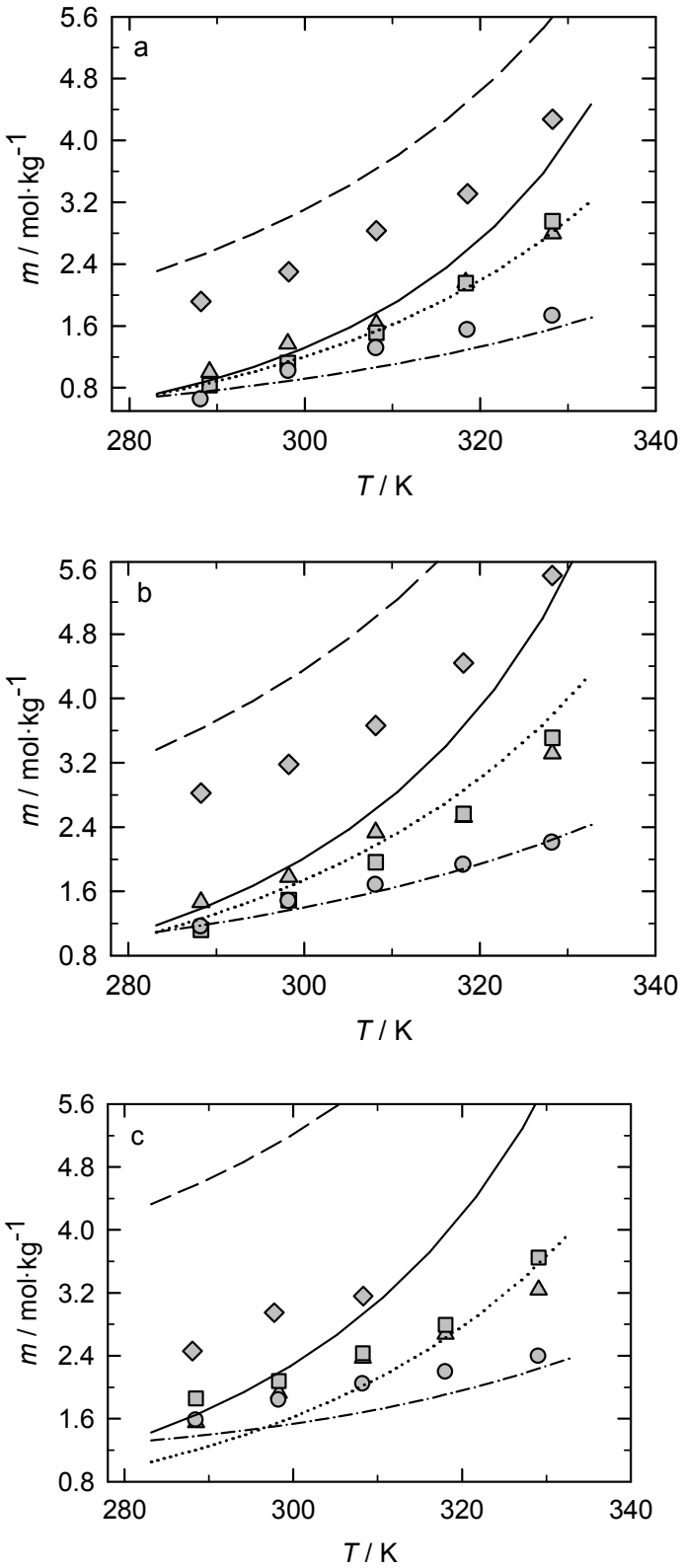

Figure 8

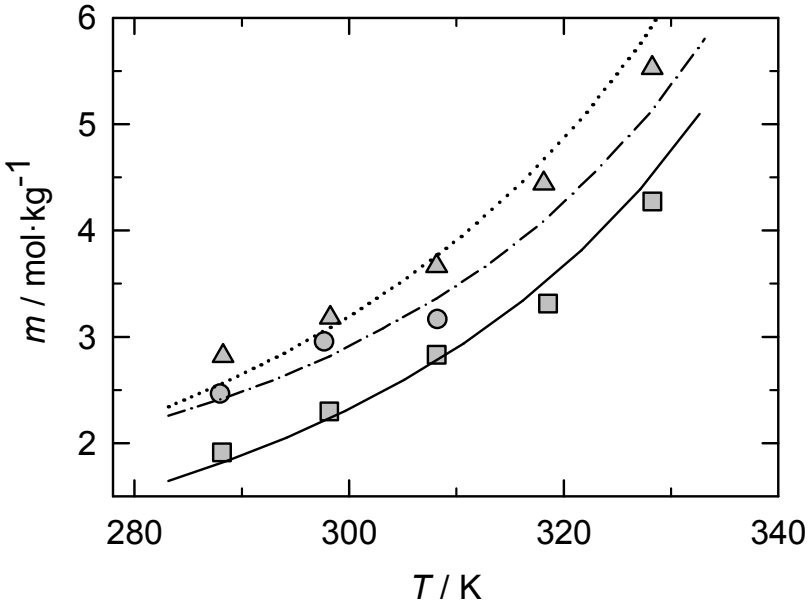

Figure 9

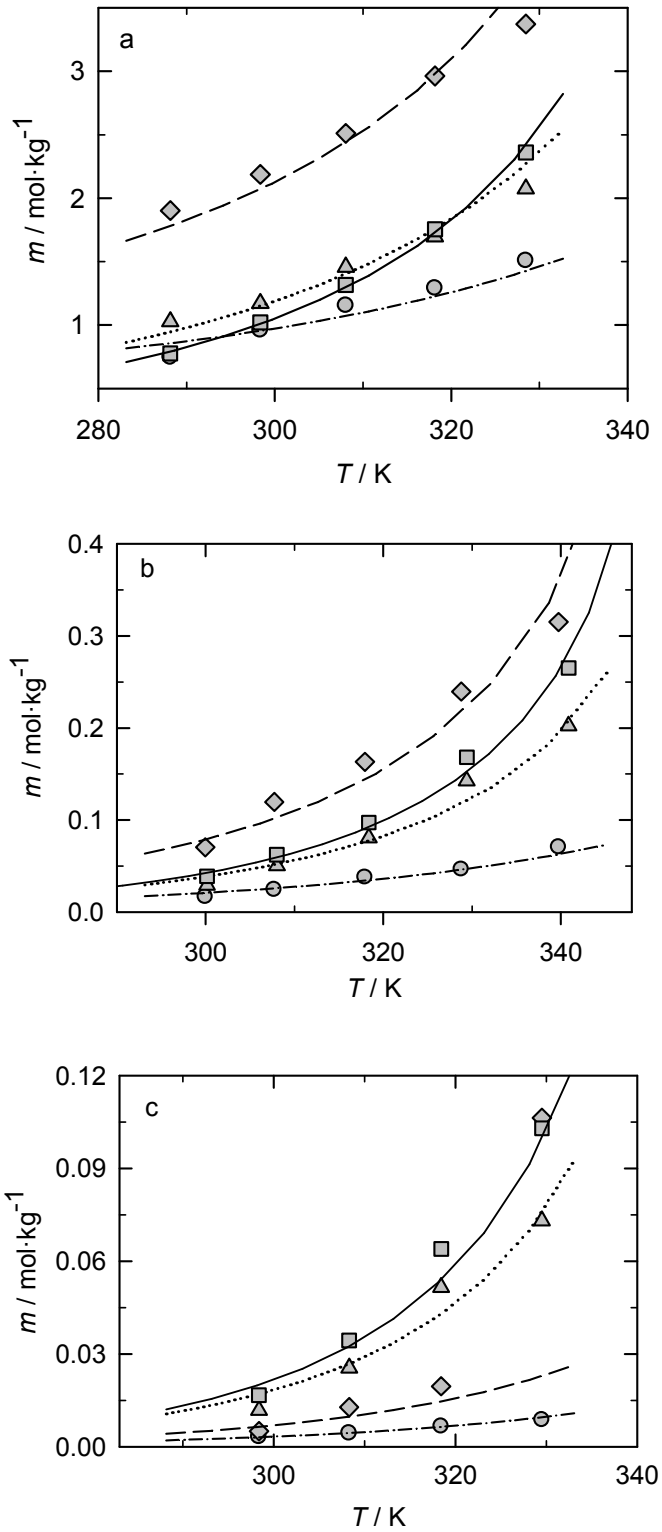

Figure 10

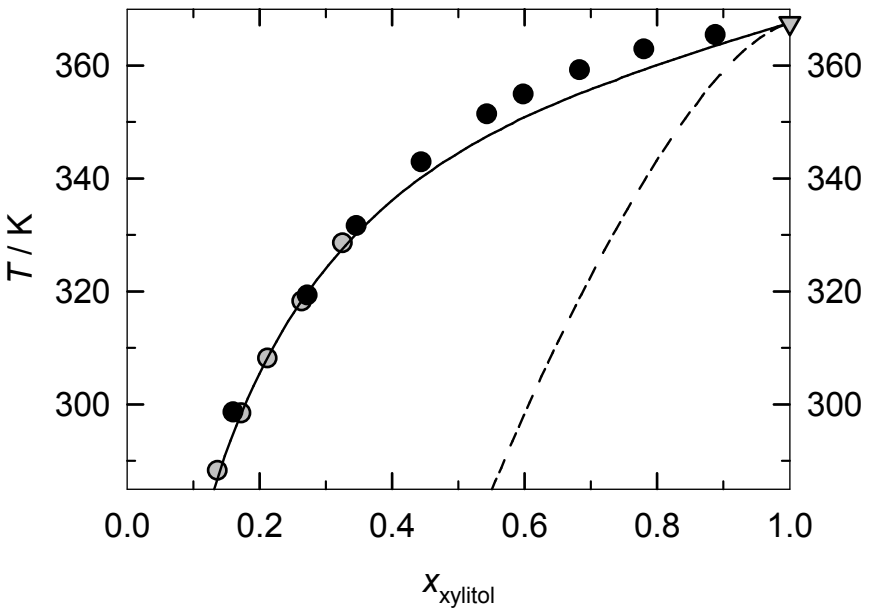

Figure 11

List of Tables

Table 1. Pure-sugar PC-SAFT parameters and their melting properties.

solute	N^{sites*}	m_i^{seg}	σ_i Å	u_i/k_B K	T_{0i}^{S-L} K	ΔH_{0i}^{S-L} kJ·mol^{-1}	$\Delta c_{p,i}^{S-L}$ J·mol^{-1}·K^{-1}
glucose	5+5	6.620	2.994	244.53	423.2[56]	32.43[57]	119.7[58]
fructose	5+5	7.387	2.849	237.19	378.2[56]	26.03[59]	98.9[31]
xylitol	5+5	6.249	2.912	242.24	367.5[60]	33.68[60]	77.3[60]
sorbitol	6+6	7.230	2.961	226.94	384.0[61**]	32.00[62]	28.08[62]

* N acceptor association sites + N donor association sites

**Value fitted to solubility in water in a previous work[35] with less than 4% deviation from experimental value[61]

association-energy parameter ε^{AiBi}/k_B = 5000 K for all sugars

association-volume parameter κ^{AiBi} = 0.1 for all sugars

Table 2. Pure-IL PC-SAFT parameters fitted to pure-IL densities and $\gamma_{1-\mathrm{p}}^{\infty}$ data (strategy 1) as well as ARD values calculated with these parameters and references for experimental data.

Ionic liquid	N^{sites*}	m_i^{seg}	σ_i / Å	u_i/k_B K	ε^{AiBi}/k_B K	κ^{AiBi}	ARD ρ[a] %	ARD γ_{1-p}^{∞} %
[emim][$EtSO_4$]	5+5	4.570	4.126	339.52	5000	0.1	0.14 [25,66-70]	6.2[71]
[emim][DCA]	4+4	3.910	4.090	358.99	5000	0.1	0.22[72,73],[b]	4.7[74]
[emim][TFA]	2+2	3.693	4.266	482.79	5000	0.1	0.06[67],[b]	0.03[75]

* N acceptor association sites + N donor association sites

[a] temperature range between 278 K and 343 K

[b] this work

Table 3. Pure-IL PC-SAFT parameters and k_{ij}s between IL and xylitol fitted to pure-IL densities and xylitol solubility in the respective IL (strategy 2), as well as ARD values calculated with these parameters.

Ionic liquid	N^{sites*}	m_i^{seg}	σ_i / Å	u_i/k_B K	ε^{AiBi}/k_B K	κ^{AiBi}	$k_{ij}^{(IL\text{-}xylitol)}$	%ARD ρ[a]	% ARD $m_{xylitol}$[b]
[bmim][DCA]	5+5	2.867	4.989	518.88	5000	0.1	0.0983	0.16[76-79]	1.6
Aliquat®[DCA]	5+5	4.862	5.659	319.23	5000	0.1	-0.0476	0.32[c]	6.9
$[P_{6,6,6,14}]$[DCA]	5+5	2.859	7.153	293.89	5000	0.1	-0.1289	0.76[80]	11.2

* N acceptor association sites + N donor association sites

[a] temperature range between 278 K and 343 K

[b] solubility data in molality units

[c] density data measured in this work

Table 4. Binary interaction parameters k_{ij} between IL and sugar determined in this work.

		k_{ij}			
Strategy	ionic liquid	glucose[a]	fructose[a]	xylitol[b]	sorbitol[b]
1	[emim][EtSO4]	-0.0042*	0.0097	0.0037	-0.0026
	[emim][DCA]	-0.0007	0.0122	0.0084	-0.0002
	[emim][TFA]	-0.0040	0.0249	0.0054	-0.0031
2	[bmim][DCA]	0.0883	0.1018	0.0983	0.0929
	Aliquat[DCA]	-0.0245	-0.0203	-0.0476	-0.0476
	[P66614][DCA]	-0.0576	-0.0389	-0.1289	-0.1263

[a] fitted to solubility data of glucose and fructose in ILs from ref [26], except in [emim][$EtSO_4$], ref [22].

[b] fitted to solubility data of xylitol and sorbitol in ILs from this work , except in [emim][$EtSO_4$], ref [25].

*Discarding solubility at 288 K due to obvious experimental error

Table 5. Density data at atmospheric pressure of pure ILs measured in this work.

	ρ / g·cm^{-3}				
T/ K	*[emim][DCA]*	*[bmim][DCA]*	*[emim][TFA]*	*Aliquat®DCA*	*[$P_{6,6,6,14}$][DCA]*
278.15	1.11527	1.07354	1.30793	-	0.91120
283.15	1.11189	1.07028	1.30387	-	0.90829
288.15	1.10851	1.06703	1.29979	0.89653	0.90537
293.15	1.10506	1.06379	1.29574	0.89367	0.90243
298.15	1.10183	1.06059	1.29170	0.89081	0.89953
303.15	1.09852	1.05739	1.28769	0.88798	0.89665
308.15	1.09523	1.05422	1.28369	0.88516	0.89378
313.15	1.09195	1.05106	1.27971	0.88234	0.89091
318.15	1.08870	1.04791	1.27575	0.87953	0.88803
323.15	1.08546	1.04478	1.27180	0.87671	0.88516
328.15	1.08224	1.04167	1.26787	0.87390	0.88230
333.15	1.07903	1.03857	1.26395	0.87110	0.87944
338.15	1.07584	1.03549	1.26005	0.86831	0.87659
343.15	1.07266	1.03241	1.25616	0.86552	0.87374

Uncertainties: u(T)=0.01 K and u(ρ)=0.00001 g·cm^{-3}

Table 6. Solubility (m) of xylitol in selected ILs measured in this work.

[emim][DCA] *M=177.21 g·mol^{-1}*			*[bmim][DCA]* *M=205.26 g·mol^{-1}*			*[emim][TFA]* *M=224.18 g·mol^{-1}*		
T[x] / K	m / mol·kg^{-1}	σm[*]	T / K	m / mol·kg^{-1}	σm	T / K	m / mol·kg^{-1}	σm
288.3	1.12	0.02	288.2	0.78	0.02	288.5	1.86	0.03
298.3	1.492	0.003	298.4	1.02	0.01	298.3	2.08	0.02
308.2	1.96	0.04	308.1	1.32	0.02	308.3	2.43	0.02
318.2	2.56	0.01	318.2	1.75	0.02	318.1	2.79	0.03
328.3	3.51	0.02	328.5	2.36	0.03	329.1	3.65	0.06
u[†](m)/m			*u(m)/m*			*u(m)/m*		
0.006			0.006			0.006		

Aliquat®[DCA] *M=472.59 g·mol^{-1}*			*[$P_{6,6,6,14}$][DCA]* *M=549.90 g·mol^{-1}*		
T / K	m / mol·kg^{-1}	σm	T / K	m / mol·kg^{-1}	σm×10^{2}
300.2	0.039	0.002	298.4	0.017	0.1
308.0	0.062	0.001	308.3	0.03437	0.002
318.4	0.097	0.001	318.4	0.0639	0.03
329.4	0.168	0.003	329.5	0.1029	0.02
340.9	0.265	0.002			
u(m)/m			*u(m)/m*		
0.005			0.007		

[x]temperature uncertainty (u(T)=±0.01 K)

[*] standard deviation

[†]average relative uncertainty: $u(m)/m = \frac{1}{N_m}\sum_{i=1}^{N_m}\frac{u(m)_i}{m_i}$

Table 7. Solubility (m) of sorbitol in the selected ILs measured in this work.

[emim][DCA] *M=177.21 g·mol^{-1}*			*[bmim][DCA]* *M=205.26 g·mol^{-1}*			*[emim][TFA]* *M=224.18 g·mol^{-1}*		
T[⁑] / K	m / mol·kg^{-1}	σm[*]	T / K	m / mol·kg^{-1}	σm	T / K	m / mol·kg^{-1}	σm
288.3	1.47	0.01	288.2	1.03	0.04	288.5	1.55	0.01
298.3	1.78	0.07	298.4	1.17	0.01	298.3	1.93	0.01
308.2	2.33	0.03	308.1	1.46	0.06	308.3	2.37	0.05
318.2	2.525	0.005	318.2	1.70	0.01	318.1	2.68	0.03
328.3	3.31	0.05	328.5	2.07	0.04	329.1	3.24	0.04
u[†](m)/m			*u(m)/m*			*u(m)/m*		
0.006			0.006			0.007		

Aliquat®[DCA] *M=472.59 g·mol^{-1}*			*[$P_{6,6,6,14}$][DCA]* *M=549.90 g·mol^{-1}*		
T / K	m / mol·kg^{-1}	σm	T / K	m / mol·kg^{-1}	σm×10^{2}
300.2	0.029	0.002	298.4	0.012	0.1
308.0	0.050	0.001	308.3	0.02549	0.002
318.4	0.081	0.002	318.4	0.0516	0.08
329.4	0.143	0.001	329.5	0.073	0.1
340.9	0.202	0.002			
u(m)/m			*u(m)/m*		
0.008			0.009		

[⁑]temperature uncertainty (u(T)=±0.01 K)

[*] standard deviation

[†]average relative uncertainty: $u(m)/m = \frac{1}{N_m}\sum_{i=1}^{N_m}\frac{u(m)_i}{m_i}$

Table 8. Water content in ILs before (initial) and after solubility measurements

	Water content / wt%		
Ionic liquid	**initial**	**xylitol**	**sorbitol**
[emim][DCA]	0.16	0.25	0.23
[bmim][DCA]	0.18	0.34	0.30
[emim][TFA]	0.12	0.18	0.19
Aliquat®[DCA]	0.05	0.16	0.16
$[P_{6,6,6,14}]$[DCA]	0.52	0.49	0.51

Table 9. ARD (%) values between PC-SAFT predictions (k_{ij}=0) and k_{ij}-correlations and experimental solubility data[a] (in molality basis) for the studied systems (IL parameter estimation strategy 1). G:glucose, F:fructose, X:xylitol and S:sorbitol.

Ionic Liquid	sugar	Ref.	ARD[b] Prediction (k_{ij}=0)	ARD[b] Correlation (k_{ij} Tab. 8)
[emim][EtSO$_4$]	*G*[c]	22	14.4	3.8
	F	22	31.3	4.6
	X	25	15.5	7.0
	S	25	8.3	5.5
[emim][DCA]	*G*	26	3.7	3.3
	F	26	33.7	5.3
	X	This work	34.9	10.8
	S	This work	11.1	10.9
[emim][TFA]	*G*	26	13.6	3.5
	F	26	112.2	4.6
	X	This work	26.5	21.7
	S	This work	13.8	9.8

[a]experimental solubility data in the temperature range: 288-328K

[b] $ARD = \frac{100}{N_{data}} \sum_{i=1}^{N_{data}} \left| 1 - \frac{m_i^{PC-SAFT}}{m_i^{exp}} \right|$

[c] solubility data point at 288 K was neglected

Table 10. ARD (%) values between k_{ij}-correlated PC-SAFT modeling and experimental solubility data (in molality basis) for the studied systems (IL parameter estimation strategy 2).

IL\ sugar	glucose[a]	fructose[a]	sorbitol[b]
[bmim][DCA]	6.7	5.3	5.4
Aliquat®[DCA]	10.6	12.3	11.1
[$P_{6,6,6,14}$][DCA]	4.9	25.8[c]	17.3

[a] k_{ij} values fitted to experimental data from ref. [26] within the temperature range: 288 - 339 K

[b] k_{ij} values fitted to experimental data from this work within the temperature range: 288 -339 K

[c] solubility at 328 K was neglected

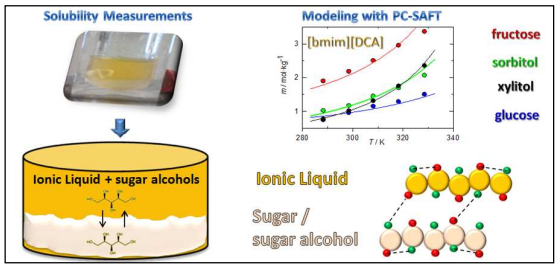
Solubility Measurements
Modeling with PC-SAFT
[bmim][DCA]
fructose
sorbitol
xylitol
glucose
Ionic Liquid + sugar alcohols
Ionic Liquid
Sugar /
sugar alcohol

TOC